Remote Sensing of Environment xxx (2011) xxx–xxx

Contents lists available at SciVerse ScienceDirect

Remote Sensing of Environment

journal homepage: www.elsevier.com/locate/rse

Evaluation of the JRC-TIP 0.01° products over a mid-latitude deciduous forest site

B. Pinty [a,b,*], M. Jung [c], T. Kaminski [d], T. Lavergne [e], M. Mund [f], S. Plummer [g], E. Thomas [c], J.-L. Widlowski [a]

[a] European Commission, DG Joint Research Centre, Institute for Environment and Sustainability, Global Environment Monitoring Unit, IES, EC Joint Research Centre, TP 272, via E. Fermi 2749, I-21027 Ispra (VA), Italy
[b] Seconded to the Earth Observation Directorate, ESA-ESRIN, via Galileo Galilei, Casella Postale 64, 00044 Frascati, Italy
[c] Max Planck Institute for Biogeochemistry, Biogeochemical Model-Data Integration Group, Hans-Knöll-Strasse 10, 07745 Jena, Germany
[d] FastOpt, Lerchenstrasse 28a, D-22767 Hamburg, Germany
[e] Center for Ocean and Sea Ice, Norwegian Meteorological Institute, Oslo, Norway
[f] Georg-August-Universität Göttingen Büsgenweg 1, D-37077 Göttingen, Germany
[g] ESA-Harwell Atlas Bldg., Harwell Science and Innovation Campus, Didcot, Oxforshire OX11 OQX, United Kingdom

ARTICLE INFO

Article history:
Received 18 May 2011
Received in revised form 22 August 2011
Accepted 27 August 2011
Available online xxxx

Keywords:
Validation
JRC-TIP
Surface albedos
LAI
FAPAR
Fluxnet
Hainich

ABSTRACT

The Joint Research Centre Two-stream Inversion Package (JRC-TIP) makes use of white sky albedo products—derived from MODIS and MISR observations in the visible and near-infrared domain—to deliver consistent sets of information about the terrestrial environments that gave rise to these data. The baseline version of the JRC-TIP operates at a spatial resolution of 0.01° and yields estimates of the Probability Distribution Functions (PDFs) of the effective canopy Leaf Area Index (LAI), the canopy background albedo, the vegetation scattering properties, as well as, the absorbed, reflected and transmitted fluxes of the vegetation canopy. In this contribution the evaluation efforts of the JRC-TIP products are extended to the deciduous forest site of Hainich (Germany) where multiannual datasets of in-situ estimates of canopy transmission—derived from LAI-2000 observations—are available. As a Fluxnet site, Hainich offers access to camera acquisitions from fixed locations in and above the canopy that are being used in phenological studies. These images qualitatively confirm the seasonal patterns of the effective LAI, canopy transmission and canopy absorption products (in the visible range of the solar spectrum) derived with the JRC-TIP. Making use of the LAI-2000 observations it is found that 3/4 of the JRC-TIP products lie within a ± 0.15 interval around the in-situ estimates of canopy transmission and absorption. The largest discrepancies occur at the end of the senescence phase when the scattering properties of the vegetation (evidenced by the pictures) and the images qualitatively confirm the seasonal patterns of the effective LAI, canopy transmission and canopy absorption products (in the visible range of the solar spectrum) derived with the JRC-TIP. Making use of the LAI-2000 observations it is found that 3/4 of the JRC-TIP products lie within a ± 0.15 interval around the in-situ estimates of canopy transmission and absorption. The largest discrepancies occur at the end of the senescence phase when the scattering properties of the vegetation (evidenced by the pictures) and the effective LAI (also derived from LAI-2000 measurements) are experiencing large simultaneous changes. It was also found that the seasonal pattern of vegetation scattering properties derived from MISR observations in the near-infrared varies together with the Excess Green index computed from the various channels of the camera data acquired at the top of the canopy.

1. Introduction

The objective of the present investigation is to evaluate the surface radiation fluxes estimated at global scale by the Joint Research Centre Two-stream Inversion Package (JRC-TIP) against in-situ observations collected at the deciduous forest Fluxnet site of Hainich (Germany). These JRC-TIP products, generated at global scale from satellite-derived surface albedo products at a spatial resolution of 0.01°, ensure the physical consistency between the suite of scattered, transmitted and absorbed radiation fluxes (this terminology will be used throughout the paper when referring to quantities normalized by the incoming radiation flux at the top of the canopy namely, albedo, transmission and absorption) in the vegetation and ground layers to ease their use and assimilation by global and regional climate models (Pinty et al., 2010a, 2010b). The partitioning between the fraction of radiation absorbed in the vegetation and ground layers in both the visible and near-infrared domains is achieved in such a way that the surface albedos (at the top of canopy) accurately fit the Moderate Resolution Imaging Spectroradiometer (MODIS) observations at 0.01° resolution including under snowy conditions. These surface products can be used by large scale models to drive

* Corresponding author at: European Commission, DG Joint Research Centre, Institute for Environment and Sustainability, Global Environment Monitoring Unit, IES, EC Joint Research Centre, TP 272, via E. Fermi 2749, I-21027 Ispra (VA), Italy.
E-mail address: bernard.pinty@jrc.it (B. Pinty).

0034-4257/$ – see front matter © 2011 Elsevier Inc. All rights reserved.
doi:10.1016/j.rse.2011.08.018

radiation as well as to constrain other processes such as those related to the water and carbon cyles. The optimal values of the retrieved state variables can also be used in conjunction with the one-dimensional two-stream radiation transfer model (Pinty et al., 2006) selected for the generation of these products in order to simulate radiation fluxes—and their partitioning—as observed.

The present contribution compares time-series measurements of the fraction of solar radiation transmitted to the background in the visible domain (0.3 μm to 0.7 μm) at the Hainich forest site against JRC-TIP generated products of this same quantity during a full vegetation seasonal cycle. Below canopy photographs, looking upwards and sideways, are used to assess product performance in relation to the timing of the growing and senescence phases. The plausibility of additional information available from the JRC-TIP about the canopy leaf scattering properties are also analyzed using series of photographs taken from a camera installed at the top of the Hainich flux tower. The benefits from operating such devices requiring limited resources to evaluate the physiological activity of the canopy have been already highlighted (see for instance, Morisette et al., 2009; Richardson et al., 2007, 2009) in particular in the context of phenology observation networks (see for instance, McNeil et al., 2008; Morisette et al., 2010; Nolan & Weltzin, 2011) (http://phenocam.sr.unh.edu).

The method and data sets selected to conduct the current evaluation exercise of the JRC-TIP products are presented in Section 2. Section 3 analyzes the patterns and quality of the JRC-TIP products with respect to information available from a series of in-situ devices. Section 4 discusses the advantages and limitations of the evaluation procedure that capitalizes on the in-situ information collected for multiple years over a number of Fluxnet sites. The current paper focuses on the case of a mid-latitude deciduous forest but the same procedure can be applied to other Fluxnet sites in order to evaluate the JRC-TIP products over various land cover conditions.

2. Method and data sets

2.1. Study area

The study area is located in the Hainich National Park, in the Thüringen region of central Germany. It is centered on a flux measurement tower, part of the CarboEurope network (http://www.carboeurope.org/) representing the European component of Fluxnet, located at 51° 04′ 45″ North and 10° 27′ 07″ East and in service since September 1999. The suboceanic–submontane climate of this 445 m plateau is characterized by a mean annual precipitation of 750 mm and a mean air temperature of 7 °C. The forested area around the tower is unmanaged, uneven-aged and largely dominated by deciduous European beech (*Fagus sylvatica*). European ash (*Fraxinus excelsior*) and sycamore (*Acer pseudoplatanus*) are co-dominant tree species and single trees of hornbeam (*Carpinus betulus*), Norway maple (*Acer platanoides*), field maple (*Acer campestris*), Scots elm (*Ulmus glabra*) and other deciduous species are admixed as remnants of a former management regime. The forest understorey is herbaceous and dominated by dog mercury (*Mercurialis perennis (L.)*) and wild garlic (*Allium ursinum (L.)*). The canopy height at the tower site is about 33 m. The tree stem diameter at breast height is on average about 0.31 m, whereas 10% of the largest trees reach 0.63 m. The largest 10% trees contribute 34% of total basal area, which amounts to 35.6 m^2/ha. The stem density was estimated at 334 per hectare in the year 2000. The bedrock is Triassic limestone covered with a loess layer of variable thickness. The brownish soils of the study area are dominantly fertile silty-clay Cambisols of 50 to 70 cm soil depth (Mund et al., 2010).

The Hainich forest is surrounded by various land cover types associated with a variety of agricultural activities (see top panel in Fig. 1) and appears spatially homogeneous over an area of at least 500 m surrounding the flux tower location (see bottom panel in Fig. 1).

2.2. In-situ observations

Our investigation uses results from LAI-2000 Plant Canopy Analyzer (LI-COR Biosciences http://www.licor.com) series of measurements available from year 2002 to 2008 along a 400 m long transect oriented in South–West direction representing the main footprint of the flux tower (Kutsch et al., 2008) (Fig. 1). The in-situ measurements were taken at 14 permanently marked sampling points along the transect, each with a distance of 30 m to the next point. Eight measurements were systematically collected around each of these sampling points. LAI-2000 measurements were taken under diffuse light conditions in the early morning, late afternoon or when the sky was cloudy. The measured fraction of transmitted radiation includes contributions from the radiation not intercepted by the vegetation elements and transmitted through the canopy gaps *i.e.*, the uncollided radiation, and the radiation that has undergone multiple scattering events within the vegetation layer as well as between the vegetation

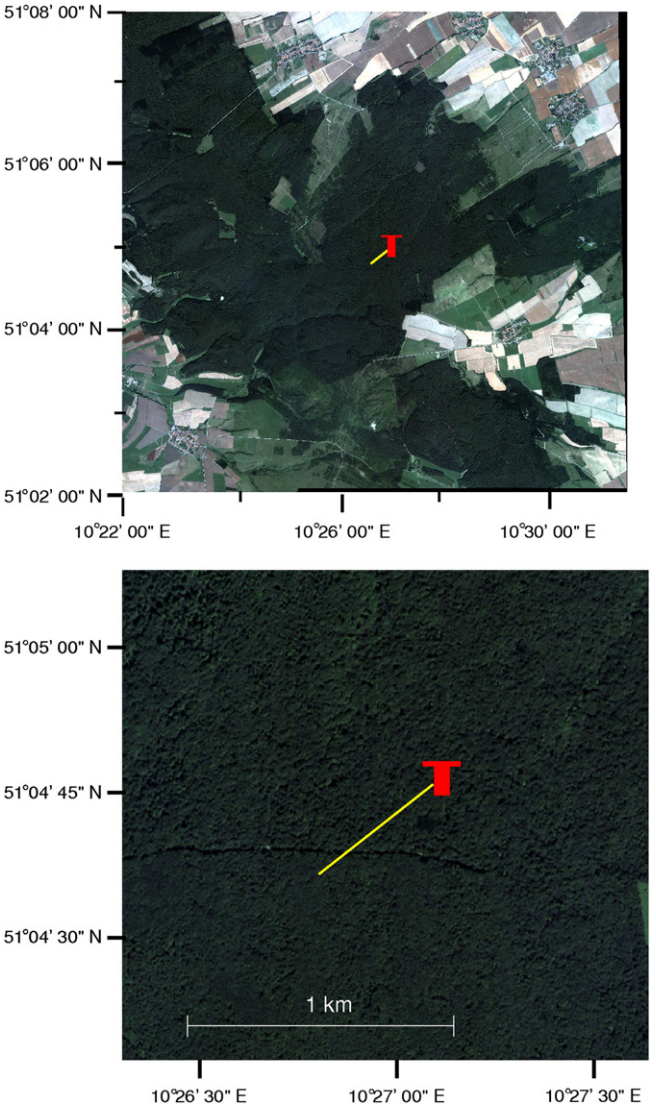

Fig. 1. The top panel shows an IKONOS image acquired on August 15, 2001 at 10:26 GMT depicting an area of about 10 × 10 km centered around the Hainich flux tower site (51° 04′ 45″ N; 10° 27′ 07″ E) identified by a red symbol. The bottom panel shows the same IKONOS image at a higher spatial resolution. The 400 m length transect selected for performing the LAI-2000 sampling is highlighted by the yellow line. (For interpretation of the references to color in this figure legend, the reader is referred to the web version of this article.)

Please cite this article as: Pinty, B., et al., Evaluation of the JRC-TIP 0.01° products over a mid-latitude deciduous forest site, *Remote Sensing of Environment* (2011), doi:10.1016/j.rse.2011.08.018

and the background. The former contribution largely dominates the latter due to the strong absorption by vegetation in the visible domain.

The diffuse transmission (also called diffuse non-interceptance) was derived using an LAI-2000 sensor located in a forest clearing (to estimate the incoming light above the forest canopy) and synchronized with another LAI-2000 sensor collecting measurements below the forest canopy along the transect. All the five available detectors (or concentric rings) were used together with a 180° view cap on both optical sensors to avoid contamination by the operator and to accommodate for the size of the forest clearing. The LAI-2000 device only accounts for radiation at visible wavelengths shorter than 0.49 μm where the canopy foliage scatters a very small amount of radiation. The estimates of diffuse transmission over the entire visible domain from this device thus tend to be slightly biased low due to the spectral variations of the canopy attributes in the 0.5 μm to 0.7 μm spectral region. The extra amount of radiation contributing to the spectrally averaged diffuse transmission in the visible domain was evaluated using the two-stream radiation transfer model (Pinty et al., 2006). This model was run with a set of canopy conditions encompassing those usually encountered at the Hainich forest site *i.e.*, green, yellow and brown leaves together with background albedo of 0.1. The bias was found to be less than 0.03 for low (<1.0) and large (>3.0) LAI and less than 0.05 for intermediate LAI conditions.

Previous investigations have highlighted the performance of a transect-based observation protocol to characterize domain-averaged vegetation quantities (see for instance, Chen et al., 2006; Gamon et al., 2006; Widlowski, 2010). Most of these studies however conclude that the estimate of domain-averaged transmitted flux quantities exhibiting limited biases and dispersion requires a much higher number of samples than is available here (and at most other sites) due to the heavy burden associated with the collection of such field measurements. The 14 independent samples collected along the 400 m transect over seven years however provide an order of magnitude of the spatial variability of the canopy transmission (using the range and interquartile range of the observed distributions).

In order to build a time series representative of a complete seasonal cycle of the forest, we opted for using together all measurements available at each 14 locations along the transect for the seven year period given that no 'exceptional' year could be identified from the selected satellite and in-situ data sets. This procedure assumes that the inter-annual variability is negligible with respect to the spatial variability occurring over the site for a given year. We applied a statistical model, namely the Random Forests algorithm from Breiman (2001), on these independent measurements using the seven year period information to generate daily measurements over a full year. The Random Forest algorithm was thus used as a gap-filler enabling us to model the spatial variability of the LAI-2000 observations at each day of year 2005 in order to ease the comparison with the satellite-derived products.

Ensembles of regression trees in Random Forests were generated with the bagging approach (Breiman, 1996) which is a bootstrapping of the training data set using random selections (sampling with replacement) of the relevant samples. With this approach, on average, about one third of the training samples are not used (so-called 'out of bag' samples) while samples from the remaining two thirds are partly replicated. Using the prediction of each regression tree for its 'out of bag' samples allows us to evaluate the cross-validation error by averaging the predicted values of the target variable for the 'out of bag' samples over all available trees and comparing that to the measured variables (this is called the 'out of bag' cross-validation). In the current application, the Random Forests algorithm was trained with 100 bagged regression trees.

A fixed digital camera (KODAK DC290) mounted on top of the flux tower at 42 m, looking North–East, provides a view across the top of the canopy. Digital images, not calibrated, are recorded automatically once a day at noon and then archived as JPEG files. This time-series of images were used to derive the Excess Green index values for year 2005. The Excess Green index was calculated from a combination of the Green (G), Red (R) and Blue (B) camera channels available as digital numbers from the JPEG files using the following formula: $ExG = 2G - R - B$ (see for instance Hufkens et al., 2011; Richardson et al., 2007; Woebbecke et al., 1995) where R, G, and B are the digital numbers normalized by the sum $R + G + B$. These digital numbers are those associated with a sub-domain in the pictures that excludes most of the sky contribution (see photos in Fig. 5). Photographs were also taken during 2005, from ground level along the 400 m transect, looking upward using a fish-eye lens to indicate the fraction of sky hidden by the forest canopy. Other photographs, looking downward at the forest floor and sideways were also systematically taken from some of the sampling points along the 400 m transect to document the state of the ecosystem at various phenological stages (Reithmaier et al., 2006).

2.3. Space derived observations

The global scale surface products were derived from the visible (0.3–0.7 μm) and near-infrared (0.7–3.0 μm) broadband white sky albedo values (equivalent to BiHemispherical Reflectances under isotropic diffuse illumination) (Schaaf et al., 2002) available from MODIS collection V005 products (MCD43B3) at 0.01° spatial resolution for successive 16-day periods (https://lpdaac.usgs.gov/lpdaac/products/modis-products-table/albedo). 'Best' and 'Good' quality flagged albedo values were considered with relative uncertainty values of 5% and 7%, respectively (Taberner et al., 2010). In addition, an absolute uncertainty limit equal to $2.5 \cdot 10^{-3}$ was set to avoid assigning too low uncertainty values in case of very low albedo values *e.g.*, over forested areas in the visible domain. The occurrence of snowy conditions was determined by the snow indicator associated with the same MODIS surface albedo 16-day period products.

The current investigation also exploits surface albedos derived from Multi-angle Imaging SpectroRadiometer (MISR) Collection 6 (generated by version 17 of the standard processor) of the MISR level 2 Aerosol and Land products (MIL2ASLS) (Martonchik et al., 1998). White sky albedo values from MISR are calculated from the land surface Bidirectional Reflectance Factor (BRF) model parameters following the angular integration and spectral conversion schemes described in Taberner et al. (2010). These BRF products, originally available in a Space Oblique Mercator projection, were first composited over 8-day periods for year 2005 using a nearest neighbor technique and then re-mapped at 0.01° resolution on a sinusoidal grid to match the one used for MODIS.

2.4. Outline of the two-stream inversion package (JRC-TIP)

The surface products are generated at global scale by operating the JRC-TIP baseline processing version (Clerici et al., 2010; Pinty et al., 2007, 2008; Voßbeck et al., 2009). This inversion scheme is based on a generic formulation of the inverse problem such that the optimal solutions result from the minimization of a cost function $J(\mathbf{X})$. The latter balances the mismatch between 1) the measured $\mathbf{d}$ (*e.g.*, MODIS or MISR visible and near-infrared broadband white sky surface albedos) and the modeled $M(\mathbf{X})$ (using the two-stream model described in Pinty et al. (2006) surface albedo with associated uncertainties specified in the covariance matrix $\mathbf{C_d}$ and 2) the deviation of the model parameters $\mathbf{X}$ from their prior values *i.e.*, the prior Probability Distribution Function (PDF) defined by mean value $\mathbf{X_{prior}}$ and covariance matrix $\mathbf{C}_{\mathbf{X}_{\mathbf{prior}}}$. The solutions are given as a Gaussian approximation of the multidimensional PDFs of the model parameters represented by a mean value $\mathbf{X_{post}}$ and a covariance matrix $\mathbf{C}_{\mathbf{X}_{\mathbf{post}}}$ documenting the uncertainties associated with these solutions at the minimum of the cost function $J(\mathbf{X})$.

Please cite this article as: Pinty, B., et al., Evaluation of the JRC-TIP 0.01° products over a mid-latitude deciduous forest site, *Remote Sensing of Environment* (2011), doi:10.1016/j.rse.2011.08.018

The cost function is thus expressed as follows:

$$J(\mathbf{X}) = \frac{1}{2}\left[\left(M(\mathbf{X})-\mathbf{d}\right)^T \mathbf{C}_\mathbf{d}^{-1}\left(M(\mathbf{X})-\mathbf{d}\right)+\left(\mathbf{X}-\mathbf{X}_{prior}\right)^T \mathbf{C}_{\mathbf{X}_{\mathbf{prior}}}^{-1}\left(\mathbf{X}-\mathbf{X}_{prior}\right)\right] \quad (1)$$

The JRC-TIP implements an inversion scheme which exploits the adjoint, tangent linear and Hessian codes of $J(\mathbf{X})$ generated by the compiler tool Transformation in C++ (TAC++) (Voßbeck et al., 2008).

The parameters $\mathbf{X}$ entering the two-stream model (Pinty et al., 2006) are, a spectrally invariant quantity, namely the effective Leaf Area Index (LAI) and, spectrally dependent parameters including 1) the true albedo of the background $r_g(\lambda)$, 2) the effective (by contrast to true) vegetation single scattering albedo, including leaves and branches, denoted $\omega_l(\lambda) = r_l(\lambda) + t_l(\lambda)$ where $r_l(\lambda)$ and $t_l(\lambda)$ refer to the effective reflectance and transmittance factors of elementary vegetation volumes, respectively, and 3) the ratio $d_l(\lambda) = r_l(\lambda)/t_l(\lambda)$ which specifies the preferential forward or backward direction of scattering in the canopy layer with respect to the source of illumination. The precise retrieval of the d_l parameter requires the unlikely condition that the observed albedos show a significant signature from the downward scattered transmission ((Pinty et al., 2004, section 3.3.3) and (Pinty et al., 2010a, section 4)). As a consequence, both the mean and one-sigma PDFs of the d_l parameter remain close to their prior values and this parameter will not be discussed further in this paper. The values taken by the 1-D model variables characterizing the vegetation canopy layer are effective in the sense that these values are derived from a 1-D homogeneous turbid medium model *i.e.*, the two-stream model, constrained to yield the same radiant fluxes as those that would be estimated from a 3-D heterogeneous canopy. The results shown in this paper use the mean retrieved values and the associated one-sigma $\sigma_{\mathbf{X}_{\mathbf{post}}}$ values as extracted from the diagonal of the covariance matrix $\mathbf{C}_{\mathbf{X}_{\mathbf{post}}}$ over one single pixel that, nominally, includes the location of the Hainich tower.

For global scale applications involving the JRC-TIP baseline processing, the prior values on the two-stream model parameters characterizing the vegetation layer are time and space invariant, *i.e.*, they are not specified as a function of land cover and/or seasons. Moreover, the effective LAI, which is largely unknown and quite variable, is specified with a very large uncertainty allowing the inversion procedure to explore any physically realistic value. The mean values $\mathbf{X}_{\mathbf{prior}}$ and associated standard deviations $\sigma_{\mathbf{X}_{\mathbf{prior}}}$ used to set the diagonal of the prior covariance matrix $\mathbf{C}_{\mathbf{X}_{\mathbf{prior}}}$ at the broadband visible (Δ_{λ_1}) and near-infrared spectral (Δ_{λ_1}) domains, respectively are the same as those adopted in earlier studies (Clerici et al., 2010; Pinty et al., 2010a) and are repeated in Table 1 for the sake of convenience. Remaining entries in $\mathbf{C}_{\mathbf{X}_{\mathbf{prior}}}$, not specified in Table 1, are set to zero.

In order to increase the computational efficiency of the JRC-TIP baseline processing version while limiting the occurrence of dubious solutions, Look-Up-Tables (LUTs) were generated in the measurement space (here a very fine discretization of the two dimensional broadband white sky albedo space) to store the JRC-TIP solutions (limited to the mean and the one-sigma PDF values of the covariance matrix $\mathbf{C}_{\mathbf{X}_{\mathbf{post}}}$) obtained off-line from selected sets of prior conditions (Clerici et al., 2010).

2.5. Space-derived versus in-situ product uncertainties

The JRC-TIP products are derived from an optimization procedure that generates Gaussian Probability Distribution Functions (PDFs) of the two-stream model parameters and the associated scattered, transmitted and absorbed radiation fluxes. The scattered and transmitted fluxes correspond to quantities that can be measured in-situ with the appropriate devices and following adequate sampling schemes in the temporal and spatial dimensions. The generation of physically consistent PDFs of these radiant fluxes *i.e.*, mean values and uncertainty ranges, constitutes a definite asset of the JRC-TIP when performing an evaluation exercise against in-situ observations. The retrieved flux uncertainties depend on the sensitivity of the simulated fluxes with respect to the model parameters and their posterior uncertainties. The latter uncertainties are, in turn, controlled by 1) the sensitivity of the (modeled) observations *i.e.*, surface albedos in the present case, with respect to the model process parameters *e.g.*, the observed albedos lack sensitivity to increasing optical depth of the vegetation layer when the latter becomes too high, 2) the observation and the radiation transfer model uncertainties, and 3) the uncertainties associated with the specification of prior information. The PDFs of the model parameters and fluxes delivered by the JRC-TIP are consistent within a Gaussian framework, consistent with the two-stream forward model, and consistent as well with the spatial resolution of the observations. In the present case they correspond to pixel/domain-averaged quantities at 0.01° resolution.

If the intra-pixel/domain (internal) variability of the land surface properties was negligible, the uncertainty associated with the in-situ local flux observations would be of the same order of magnitude as those provided by the in-situ measuring devices *e.g.*, a few percent relative for the transmitted fluxes. These uncertainties would thus be systematically smaller than those associated with the retrievals from space observations. The latter uncertainties reflect the limited amount of information on the vegetated surfaces provided by albedo observations even if they were very accurate. Unfortunately, the internal variability characterizing most land surfaces at 0.01° spatial resolution induces a rather intricate situation (see for instance, Baldocchi & Collineau, 1994; Chen et al., 1997a; Law et al., 2001).

This sub-pixel scale variability arises due to three-dimensional variations in leaf density as well as leaf and vegetation background radiative properties. The accurate and precise estimates of pixel/domain-averaged flux values from in-situ devices depend on the level of statistical variability prevailing in the vegetation canopy (see Gobron et al., 2006 for an attempt to categorize this variability in three different radiation transfer regimes). Adequately accounting for such statistical variability at multiple spatial resolutions with ground based devices is the crux of the matter when comparing space-derived pixel/domain-averaged against an ensemble of in-situ local observations (see for instance, De Kauwe et al., 2011; Morisette et al., 2006; Reifsnyder et al., 1971; Widlowski, 2010). If and when this is achieved in the best possible manner, one ends up with a series of measurements that sample, for a given pixel, the PDF expressing the internal variability of the fluxes. By contrast, the JRC-TIP derived PDFs refer to domain-averaged quantities. It should be noted that the width of in-situ derived PDF is thus not controlled by the same processes as those involved in establishing the uncertainty of the JRC-TIP retrievals. In this study, the interannual variability is also included in the in-situ uncertainties.

3. Results and discussion

3.1. MODIS and MISR white sky albedos

Fig. 2 displays the time series of the broadband white sky albedos from MODIS (red) and MISR (blue) in the visible (top panel) and near-infrared (middle panel) domains. These observed albedo values are used as input to the JRC-TIP and, in practice, indiscernible from the posterior albedo values reconstructed using the optimally retrieved model parameter values. The one-sigma uncertainty of the latter (extracted from the posterior covariance matrix) and represented by vertical bars around the mean of the PDF values in the two top panels in Fig. 2) remains well below the prescribed uncertainty range of the observations (specified in $\mathbf{C}_\mathbf{d}$ in Section 2.4).

In general, the MISR derived albedos values tend, in both spectral domains, to be higher than those from MODIS along the season. Some Winter time observations *e.g.*, in January and February, deviate significantly, probably due to ephemeral snow events contaminating the

Please cite this article as: Pinty, B., et al., Evaluation of the JRC-TIP 0.01° products over a mid-latitude deciduous forest site, *Remote Sensing of Environment* (2011), doi:10.1016/j.rse.2011.08.018

MISR daily observations. Both sets of near-infrared observations suggest a well-marked seasonal trend as can be expected over a deciduous forest due to the strong absorption of visible radiation by the changing density of green leaves and hence increased scattering in the near-infrared domain (see for instance, Pinty et al., 2009). The observed temporal trend in albedo through the year thus corresponds to the expected forest phenology.

The values of the cost function (bottom panel in Fig. 2) given by Eq. (1) and associated with the retrievals remain low and mainly below 0.5 in all cases but one occurring at the end of February (during the period from February 18 to March 5, 2005) identified by open diamond symbols (on the two top panels) where it exceeds 1.5. The latter is associated with high surface albedo values in the visible domain from both sensors and relatively low values in the near-infrared. These observations are probably contaminated by snow but not flagged as such in the MODIS 0.01° resolution product for this particular pixel. Most of the surrounding pixels are however flagged as snow for this time period and the probability of having snow contaminated conditions over this particular pixel is thus relatively high. Given that the prior information on the background properties turns out to be probably erroneous on that particular date, snow free versus snowy conditions (see Table 1) the JRC-TIP returns a relatively high cost function value due to the significant deviations of the retrieved background albedo values in the visible from the prior values (Pinty et al., 2008) (see Section 3.4 for the snow corrected solutions). Despite the high cost function value, the JRC-TIP still provides posterior albedo values that fit those observed well.

3.2. JRC-TIP transmission against ground-based estimates

The time-series of the fractions of radiation transmitted through the Hainich forest site to the ground derived from the in-situ LAI-2000 devices are shown in Fig. 3 (top panel). The observed values at each of the 14 locations along the 400 m transect (indicated by the plus (+) symbol) at different dates of the year are used to evaluate the range (light gray shaded zone) and the interquartile range (dark grey shaded zone) after applying the statistical interpolation model. The 'out of bag' cross-validation procedure delivers a root mean square error of 0.05 for the fraction of transmitted flux. The actual in-situ observations specifically available for year 2005 at days 141, 150, 157 and 283 are identified in yellow and by downward arrows.

The overall seasonal pattern resembles an inverted hat shape with a fast growing season starting during the second half of April (from Day of Year (DOY) 110–115) associated with a strong decrease in the fraction of transmitted light. Then, from around mid-May (DOY 135–140) to mid-October (DOY 285–290) the in-situ observations stay at about the same low level, that is, between 0.05 and 0.1 suggesting a dense canopy cover during this time period. Following that, the values estimated from the in-situ measurements increase up to 0.75–0.8 (with an interquartile range of about 0.1) and are close to those observed before the start of the growing season. Note that the staircase pattern discernible during the senescence phase is due to the limited number of LAI-2000 measurements that are available for this critical phenological stage (*i.e.*, data from year 2007 only). One may also notice the broadening of the statistical range from approximately 0.2–0.25 associated with the dormant season to values between 0.3 and 0.4 during the mature phase. During the mature phase, the canopy gaps induce a large possible range of values of the fraction transmitted radiation and contribute more efficiently to the dispersion of the in-situ observations, a signature of the sub-pixel/domain spatial variability.

On the same panel, the time-series of the pixel/domain-averaged fraction of transmitted radiation derived from applying the JRC-TIP on the MODIS (in red) and MISR (in blue) white-sky albedos presents a relatively smooth profile. The contamination by snow of the MISR albedos until end of February (DOY 49–56) (see Fig. 2) is responsible for the excess of transmitted flux. The selection of the false prior background albedo is such that no contribution from the vegetation layer (even from woody elements) is required to fully interpret the MISR albedos. The same reasoning applies also to the MODIS based retrievals in February (periods covering data from DOY 33 to DOY 64) that are not flagged as 'best' quality products. (The values of the model process parameters and the radiation fluxes retrieved under conditions where the background is assumed to be partly snowy (see Table 1) are displayed in Figs. 4 and 7 and described in Section 3.4). From the beginning of March to the end of August, the agreement between both MODIS and MISR derived values and the in-situ observations is good given the uncertainties associated with both categories of products. The high bias of the satellite derived products, especially during the mature phase, is due to the well-known radiation saturation phenomenon occurring in the visible spectral range over dense canopies *i.e.*, adding more absorbing leaves on trees changes neither the transmitted flux nor the flux scattered to the satellite significantly. In this period, both uncertainty ranges are large indicating the presence of rather wide PDFs for the various reasons outlined in Section 1.

The largest systematic discrepancy between the satellite derived and in-situ estimates of transmission occurs during the senescence phase. The satellite values are biased high and this bias is equivalent to a time lag of approximately ten to fifteen days. During this senescence period, the values retrieved from both MODIS and MISR show a good agreement and a noticeable temporal consistency. By contrast, the fraction of transmitted radiation measured with the LAI-2000 during DOY 283 in year 2005 (yellow) indicates, unlike the satellite retrievals, that the canopy is still able to intercept a large amount of radiation. This disagreement can thus hardly be associated with the temporal under-sampling of this period by in-situ observations but rather with changes in the scattering properties that will be addressed in greater detail in Section 3.6. The anomalous MODIS derived value at the beginning of August (DOY 209 to 224) is probably due to local cloud contamination that translates into a local increase in the visible albedo product (see Fig. 2). Note also that this observation is not associated with the 'best' quality flag value.

3.3. JRC-TIP extinction and absorption against ground-based estimates

A specific JRC-TIP scenario was designed to estimate effective LAI values on the basis of the in-situ measurements of transmission as the only observation set with a prescribed uncertainty of ± 0.05 to each individual observation. The prior values were as specified in Table 1.

The middle panel in Fig. 3 displays these effective LAI values (with the plus (+) symbols) corresponding to the fraction of total transmission under diffuse sky illumination estimated in-situ along the 400 m transect with the LAI-2000, together with the associated range (light grey shaded zone) and interquartile range (dark grey shaded zone). The continuous time-series was generated from the Random Forests algorithm operated under the same conditions as described in Section 2.2 and the 'out of bag' cross-validation procedure yielded a root mean square error of 0.32.

The very large differences in effective LAI from the satellite-derived and in-situ products during the phase of maturity illustrate the saturation phenomenon in the visible light attenuation process: variations by almost a factor 1.5 in the median values (from about 3 from the satellite derived albedos to 4.5 from the in-situ transmissions) correspond to variations between approximately 0.05 (measured in-situ) and 0.1 (generated from the albedo observations) in the fraction of transmitted radiation (see top panel in Fig. 3). The large uncertainty of the effective LAI values retrieved from the albedo observations attests of the very limited sensitivity of the scattered signal to this model parameter beyond values of about 3.0. Effective LAI values reaching 3.0 or slightly higher thus represent an upper bound of the mean of the PDF for the JRC-TIP retrievals delivered by the baseline processing *i.e.*, when using albedo observations as input and the conditions discussed in (Pinty et al., 2010a) regarding the prior values and observational uncertainties.

Please cite this article as: Pinty, B., et al., Evaluation of the JRC-TIP 0.01° products over a mid-latitude deciduous forest site, *Remote Sensing of Environment* (2011), doi:10.1016/j.rse.2011.08.018

Table 1
Mean values $\mathbf{X_{prior}}$ and associated standard deviations $\sigma_{\mathbf{X_{prior}}}$ used to set the diagonal of the prior covariance matrix $\mathbf{C_{X_{prior}}}$. Δ_{λ_1} and Δ_{λ_2} correspond to the broadband visible (0.3–0.7 μm) and near-infrared (0.7–3.0 μm) spectral domains, respectively. $\omega_l(\Delta_{\lambda_{1,2}})$, $d_l(\Delta_{\lambda_{1,2}})$ and $r_g(\Delta_{\lambda_{1,2}})$ refer to the effective canopy single scattering albedo, asymmetry factor and background albedo, respectively.

Variable identification	$\mathbf{X}_{prior}$	$\sigma_{\mathbf{X_{prior}}}$
LAI	1.5000	5.0
$\omega_l(\Delta_{\lambda_1})$	0.1700 and 0.1300[a]	0.1200 and 0.0140[a]
$d_l(\Delta_{\lambda_1})$	1.0000	0.7000
$r_g(\Delta_{\lambda_1})$	0.1000[b] and 0.50[c]	0.0959[b] and 0.346[c]
$\omega_l(\Delta_{\lambda_2})$	0.7000 and 0.7700[a]	0.1500 and 0.0140[a]
$d_l(\Delta_{\lambda_2})$	2.0000	1.5000
$r_g(\Delta_{\lambda_2})$	0.1800[b] and 0.350[c]	0.2000[b] and 0.25[c]

[a] Value associated with the 'green' leaf scenario.
[b] Value adopted for the bare soil case with a correlation factor between the two spectral domains of 0.8862 set in $\mathbf{C_{X_{prior}}}$.
[c] Value adopted under occurrence of snow with a correlation factor between the two spectral domains of 0.8670 set in $\mathbf{C_{X_{prior}}}$.

With a specified uncertainty of ±0.05 on the input transmission values, the JRC-TIP returns uncertainties (the one-sigma PDF) of approximately 0.15, 0.5 and 1.75 for effective LAI values of 1.0, 3.0 and 5.0, respectively. These uncertainty values contrast with the statistical range of effective LAI values (the light grey zone in Fig. 3) that is due to spatial variability along the 400 m transect and with those that are associated with the JRC-TIP baseline set up that uses MODIS and MISR albedo as input observations (see also section 4.1 in Pinty et al., 2010a). It must be recalled here that, for both inverse scenarios, the reported uncertainties are internally consistent according to the inverse procedure summarized in Section 2.4.

The time-series of the fraction of radiation absorbed by the vegetation layer in the visible domain retrieved from the JRC-TIP when using the observed MODIS and MISR albedos is shown in Fig. 3 (bottom panel). These values are displayed together with the in-situ intercepted fraction (that is, the [1 − T] quantity where T denotes the fraction of transmitted radiation) displayed in the top panel. The continuous time-series was generated from the Random Forests algorithm operated under the same conditions as described in Section 2.2 and the 'out of bag' cross-validation procedure yielded a root mean square error of 0.05. The satellite-derived and in-situ data sets exhibit a rather good agreement up to the onset of the senescence phase, except for the snow related conditions discussed previously that contaminate the MODIS and MISR surface albedo products.

The capability of the intercepted fraction to approximate the fraction of absorbed radiation in the visible domain within ±0.1 precision limit has been evaluated in previous analytical (see section 2.7.2 in Pinty et al., 2006), (see section 4.2 in Gobron et al., 2006) and numerical modeling investigations (Pinty et al., 2009; Widlowski, 2010). It basically results from the high probability of absorption by plant canopies with the associated low effective single scattering albedo and a negligible contribution from the background. Any departure from these basic conditions introduces some bias in the quality of the approximation of the absorbed fraction using interception: Pinty et al. (2010c) highlighted the contribution of strongly backscattering snowy backgrounds that enable the vegetation layer to absorb more radiation than is possible from the interception of the downward solar radiation while Widlowski (2010) estimated the systematic biases introduced on this approximation by varying leaf properties *i.e.*, leaf single scattering albedos.

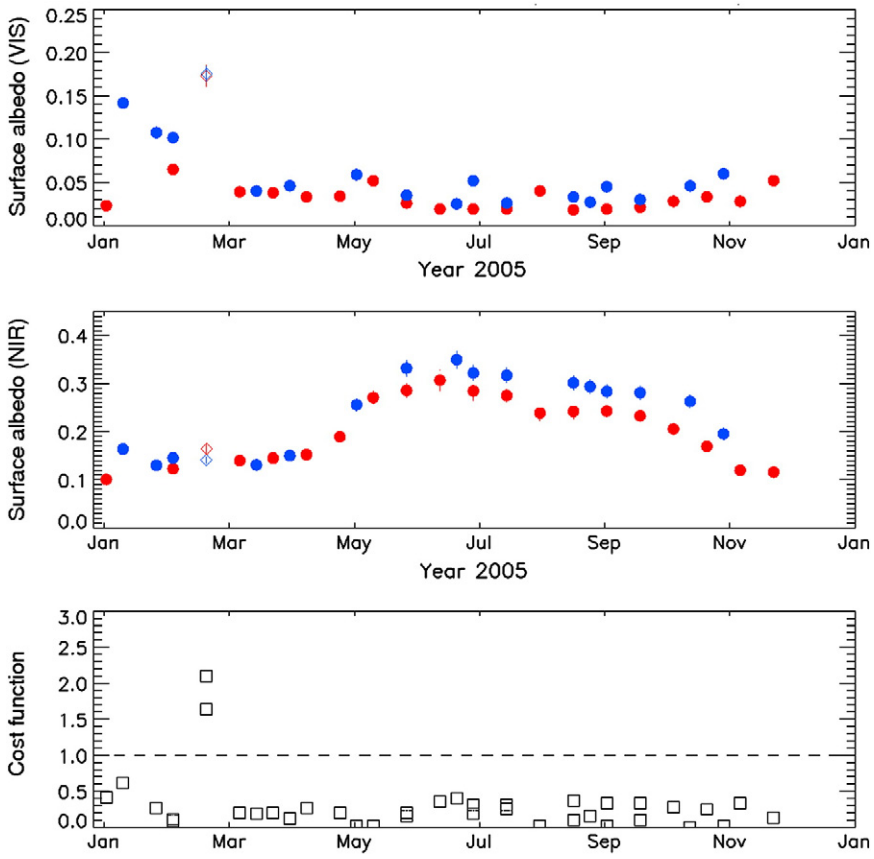

Fig. 2. Time series of the broadband BHR–white sky–surface albedo at 0.01° spatial resolution in the visible (top panel) and near-infrared (middle panel) domain over the site of Hainich (51° 05′ 05″ N; 10° 26′ 41″ E). MODIS (MISR) derived albedo values are featured in red (blue). High cost function values (bottom panel) are identified with an open diamond symbol. The vertical bars display the one-sigma posterior uncertainty values. (For interpretation of the references to color in this figure legend, the reader is referred to the web version of this article.)

Please cite this article as: Pinty, B., et al., Evaluation of the JRC-TIP 0.01° products over a mid-latitude deciduous forest site, *Remote Sensing of Environment* (2011), doi:10.1016/j.rse.2011.08.018

The bias identified in Widlowski (2010) is such that the intercepted fraction exceeds the absorbed fraction that is, leaves of different colors contribute indiscernibly to the interception process (which is a process driven by canopy structure) while their absorption probabilities depend on their chlorophyll content (which is a biochemically driven process). Based on computer simulations of European beech forests, Widlowski (2010) indicated a bias of 0.07 and 0.1 in the fraction of absorbed radiation if the foliage is yellow and brown, respectively. This deficit in absorption may partly contribute to the observed deviations shown in the bottom panel of Fig. 3. This same figure suggests, however, that larger deviations are likely to occur at the onset of the senescence phase, probably due to the concurrent changes in the effective LAI.

3.4. Qualitative evaluation of the JRC-TIP retrievals

Fig. 4 displays the time-series of the fractions of radiation transmitted to the ground (top panel, same data points as shown in Fig. 3) and absorbed in the visible domain (bottom panel) as derived by the JRC-TIP using the MODIS (in red) and MISR (in blue) white-sky albedos as inputs. The middle panel shows the seasonal cycle of the main controlling parameter namely the effective LAI retrieved by the JRC-TIP. The vertical bars indicate the one-sigma values of the retrieved PDFs under conditions where the input albedos are flagged as being of 'best' (solid) and 'good' (dashed) quality. The JRC-TIP values retrieved using the prior conditions associated with a snowy background are shown with open symbols at the dates indicated with the open triangles. Images taken with an upward looking direction are shown in the upper half of the figure while images of the forest floor are displayed in the lower half of the figure.

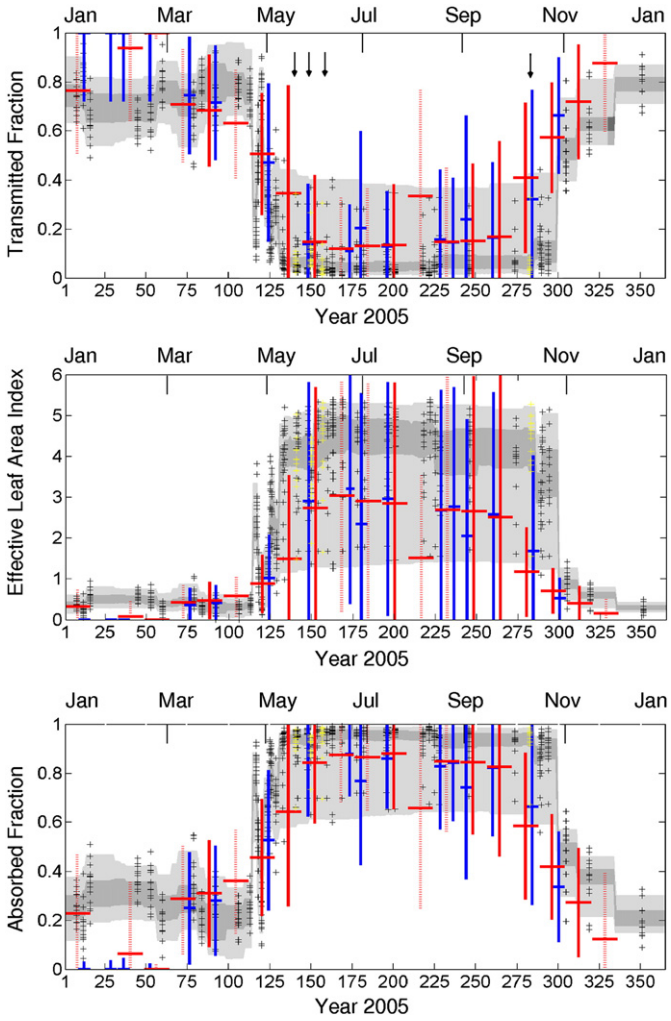

Fig. 3. Top panel: Time series of the domain-averaged fractions of diffuse transmission in the visible spectral domain measured over the Hainich site. The grey shaded zones indicate the range (light grey) and interquartile (dark grey) range estimated both from the individual sampled points over all seven years (black crosses). The points available in 2005 at dates indicated by the downward arrows are shown with yellow crosses. The JRC-TIP derived estimates from MODIS (MISR) are shown in red (blue). The full (dashed) vertical bars indicate the one-sigma posterior uncertainty associated with the best (good) quality MODIS input albedos. Middle and bottom panels: same as above except for the effective LAI and the fraction of absorbed flux in the vegetation layer, respectively. (For interpretation of the references to color in this figure legend, the reader is referred to the web version of this article.)

The pictures on April 1st (DOY 91) indicate that the deviation from unity of the fractions of transmitted radiation is due to the woody attributes of the forest only. Here, the leaf-free structure of the trees translates into an effective LAI around 0.5. On May 10 (DOY 130), the presence of green leaves is already quite significant and their density increases further as can be observed on photos taken on July 19 (DOY 200) and August 30 (DOY 242), when the masking of the sky appears to reach a maximum. This time sequence thus seems consistent with the smooth temporal variations exhibited by the JRC-TIP retrievals. One can note that the adoption of snowy background as a prior condition, during the dormant season in January and February, yields more credible results in all three quantities displayed in Fig. 4 (closed to open symbols).

Some subtle changes *i.e.*, yellowing, are discernible on both the upward looking and sideview pictures on October 18 (DOY 291). The masking of the sky does not, however, seem to be affected yet corroborating thus the in-situ LAI-2000 estimates of the transmitted light (see yellow symbols on top panel in Fig. 3). The forest appears to experience a rapid change in the following days as attested by the photos available on October 25 (DOY 298) where one can notice a more definite yellowing and browning of the leaves with a reduced leaf density.

The leaf optical properties, expressed through the effective single scattering albedo of the vegetation layer, can be evaluated during the mature stage of the forest, that is, when the effective LAI is large enough to favor the retrieval of vegetation scattering properties with a posterior uncertainty smaller than its prior value (for further detail see section 4.3 in Pinty et al., 2010a). Fig. 5 indicates that such favorable conditions occur from about May until mid-October. All pictures shown in this figure are taken from the top of the canopy. The picture available on May 10 (DOY 130) shows the presence of young green leaves and contrasts with the situation on April 1st (DOY 91) where only woody elements can be seen. The canopy greening appears to consolidate by the end of June according to the JRC-TIP results: the effective single scattering albedo decreases in the visible (bottom panel) and simultaneously increases in the near-infrared domain (top panel). Such a variation indicates an enhanced probability of absorption (scattering) by vegetation in the visible (near-infrared) domain that is most likely associated with the greenness of the young leaves. From July to September, one can observe the reverse of this trend in the near-infrared domain which could be attributed to processes associated with the aging of the leaves (see for instance Gausman & Allen, 1973; Knapp & Carter, 1998; Ollinger et al., 2008; Roberts et al., 1998). The picture taken on August 30 (DOY 242) suggests that the light green associated with young leaves has indeed evolved into a darker green. The yellowing/browning of the vegetation canopy is very discernible from the picture taken on October 18 (DOY 291). In-situ observations indicate that the co-dominant tree species add some variability in the leaf coloring and senescence behavior. The changes occurring in the vegetation in autumn appear better established on the October 25 (DOY 298) picture.

As expected, the small differences between MODIS versus MISR albedos affect directly the retrieved vegetation scattering properties when the effective LAI is large enough to mask the background signature. The MODIS and MISR retrievals covary but with a noticeable bias between the retrieved values (in the range 0.03–0.05 in the visible and 0.05–0.07 in the near-infrared domain, respectively) that mirror

Please cite this article as: Pinty, B., et al., Evaluation of the JRC-TIP 0.01° products over a mid-latitude deciduous forest site, *Remote Sensing of Environment* (2011), doi:10.1016/j.rse.2011.08.018

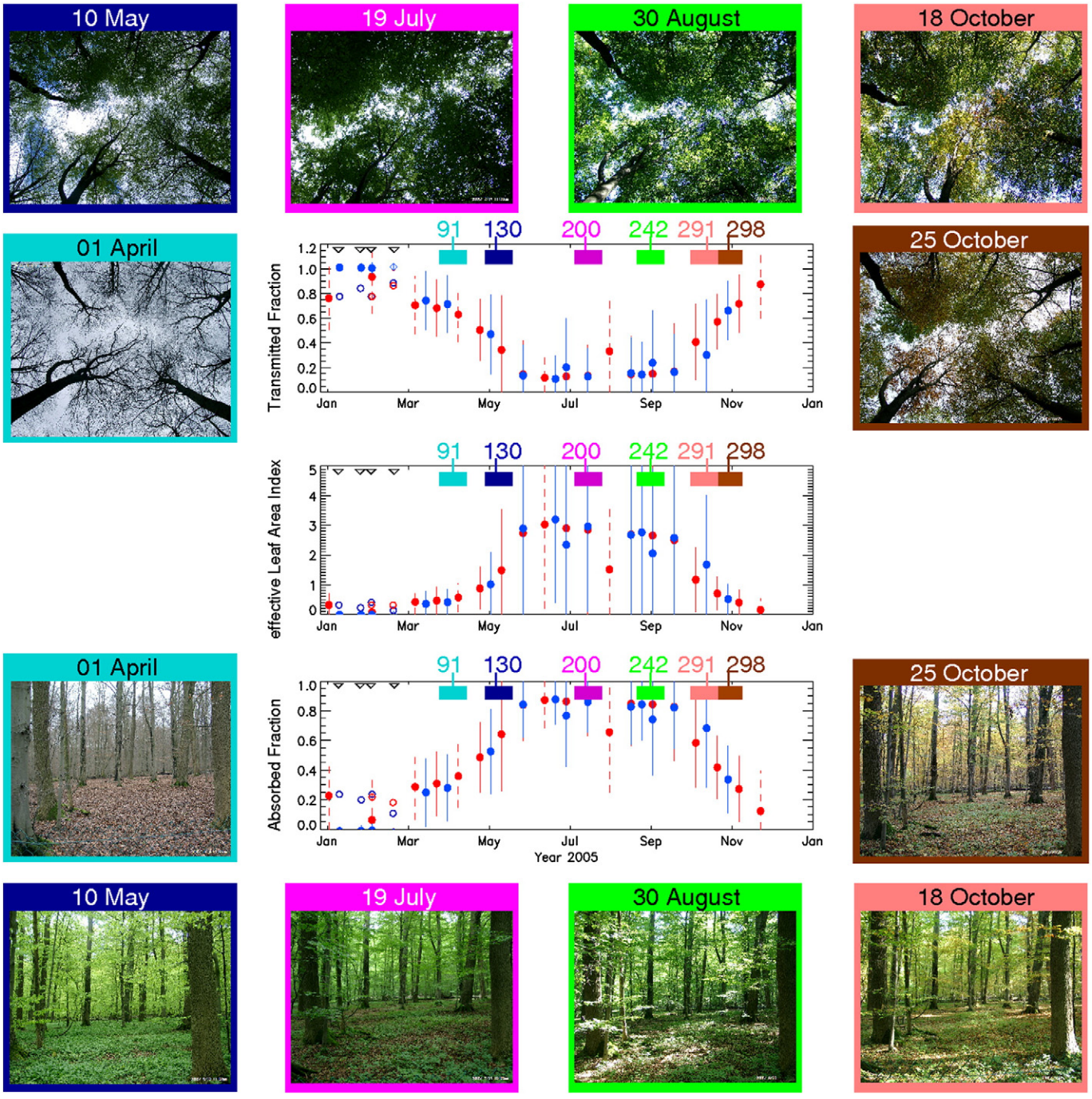

Fig. 4. Time series of the fraction of the transmitted (top panel) and absorbed (bottom panel) radiation in the visible domain estimated by the JRC-TIP. The corresponding effective LAI is shown in the middle panel. Symbols and color coding are the same as in Fig. 2. The full (dashed) vertical bars indicate the one-sigma posterior uncertainty associated with the best (good) quality MODIS input albedos. Open symbols are for the mean of the PDFs retrieved assuming a snowy background at dates identified by triangles on the top axis. Hemispherical (lateral) views of the canopy taken below the canopy are displayed in the upper (lower) part of the figure. The dates of the photos are color coded and identified in the three inside panels. (For interpretation of the references to color in this figure legend, the reader is referred to the web version of this article.)

the differences in the input albedo values (see Section 3.1). Despite these differences related to the input observations, the JRC-TIP retrieves unique information about pixel/domain-averaged scattering properties of the vegetation layer and this seems to be confirmed by the photos taken from the top of the canopy *i.e.*, with no contamination by the background.

Fig. 6 illustrates the relationship between the effective single scattering albedo retrieved in the near-infrared domain (top panels) and the Excess Green Index (ExG) (bottom panel) derived from the series of pictures taken by the tower camera during year 2005. The ExG index shown in Fig. 6 has been temporally smoothed with a ten day running average to emphasize the dominant seasonal patterns of this greenness index. The ExG index consistently takes low values during the season of dormancy that is in the absence of green phytoelements (approximately before day 125 and after day 300). It increases to relatively large values between day 150 and day 175 due to the scattering by green leaves that enhance the relative contribution of the green channel to the ExG index as compared to the red and blue channels. The ExG index then decreases slowly until day 300 where it reaches low values typical of the dormant season.

Please cite this article as: Pinty, B., et al., Evaluation of the JRC-TIP 0.01° products over a mid-latitude deciduous forest site, *Remote Sensing of Environment* (2011), doi:10.1016/j.rse.2011.08.018

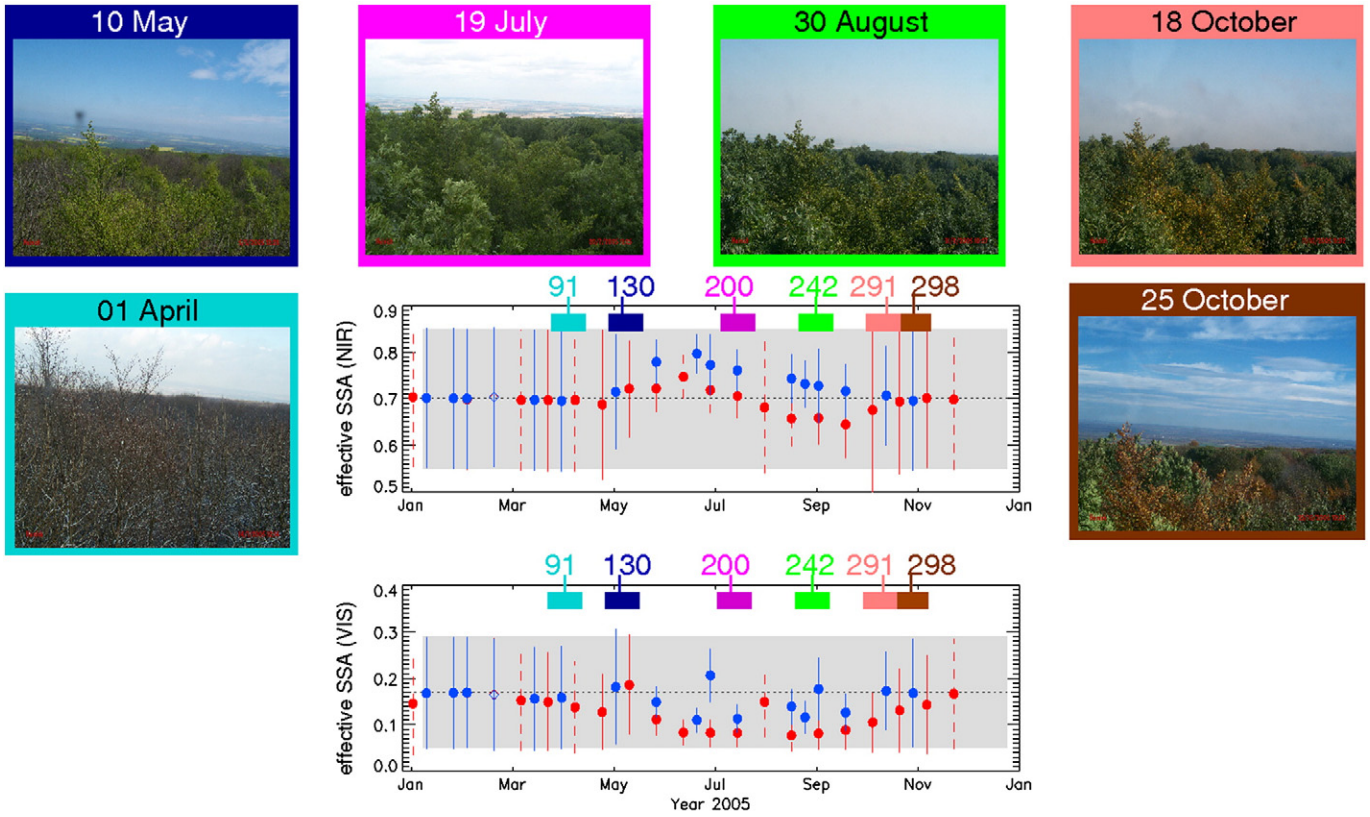

Fig. 5. Time series of the effective canopy single scattering albedo inferred in the near-infared (top panel) and visible (bottom panel) estimated by the JRC-TIP. Symbols and color coding are the same as in Fig. 2. The shaded zones delineate the one-sigma prior uncertainty values. The full (dashed) vertical bars indicate the one-sigma posterior uncertainty associated with the best (good) quality MODIS input albedos. Photos of the top of the canopy taken from the tower are displayed in the upper part of the figure. The dates of the photos are color coded and identified in the two inside panels.

This decrease appears to occur at a faster rate from day 175 to day 220 than in the remaining period. Fig. 6 shows that the variations in the retrieved near-infrared effective single scattering albedos follow very closely the ExG index patterns especially in the case of the MISR retrievals (middle panel). The effective single scattering albedos, not resolved precisely during the dormant season (due to limited leaf density), are associated with the ExG minimum value. The deviations of the ExG index from its minimum concur with satellite retrievals whith concomitant uncertainties that are much less than their prior values (see Table 1). The large effective single scattering albedos occur at the end of the green-up period marked by relatively large ExG index values. This maximum green canopy condition yields single scattering albedo values that are quite close to the mean of the prior PDF adopted for the JRC-TIP 'green' leaf scenario (see Table 1). Finally, the seasonal variations observed in retrieved single scattering albedo during the growing and mature phases are strongly correlated with those exhibited by the ExG index. This suggests that the effective single scattering albedo retrieved from MISR in the near-infrared domain includes the signature of processes related to the aging of the leaves.

Photos of the typical background are displayed in Fig. 7 together with the JRC-TIP retrieval of its albedo values in the visible and near-infrared domains. By contrast with the retrieval of leaf optical properties, high effective LAI values prevent a precise estimate of the background albedo from the available MODIS and MISR albedos. The reduction of the posterior uncertainties with respect to their prior values, indeed, occurs from January to April and mid-October to end of the year. The JRC-TIP solutions obtained using prior conditions corresponding to a snowy background (shown with open symbols) show an increase (decrease) in the visible (near-infrared) domain, as compared to the snow-free conditions. None of the situations where the understory is characterized by the presence of small green leaves can actually be precisely evaluated from JRC-TIP retrievals due to the concurrent increase in the effective LAI of the overstory. One can notice, however, that the retrieved pixel/domain-averaged albedo values of the background get close again to their Spring values from mid-October and beyond. The differences between the MODIS versus MISR retrievals in the second half of October (two data points available) are due to differences in the input albedo values from these two data sets. In such instances, the MISR retrieved values are systematically higher than those derived from the MODIS data set. One cannot however draw conclusions from this observed bias or speculate on the comparative quality of both albedo data sets from the available in-situ information at this site. If there was an adequate spatio-temporal in-situ sampling of the background albedo values *e.g.*, at the same locations as those selected for the LAI-2000 measurements, further insight could be obtained on the cause of these differences.

3.5. Biases between the JRC-TIP and the in-situ flux estimates

The detailed analysis of the seasonal changes exhibited by the JRC-TIP products for year 2005 together with the in-situ derived information supports the assumption of 1) the presence of snow on the background during observations taken from mid-January to end of February and 2) the contamination by clouds of the MODIS albedo products at the beginning of August (DOY 209 to 224) (the open symbols in Figs. 4 and 7). Accordingly, the biases between the JRC-TIP and the in-situ fluxes were estimated using the JRC-TIP solutions retrieved with prior conditions related to a snowy background (see Table 1) for the period under 1) while the MODIS products derived at the beginning of August were dropped from the analysis.

The top panel in Fig. 8 displays the time-series of the differences between the fractions of the transmitted flux delivered by the JRC-TIP and those derived from the in-situ measurements gathered along the

Please cite this article as: Pinty, B., et al., Evaluation of the JRC-TIP 0.01° products over a mid-latitude deciduous forest site, *Remote Sensing of Environment* (2011), doi:10.1016/j.rse.2011.08.018

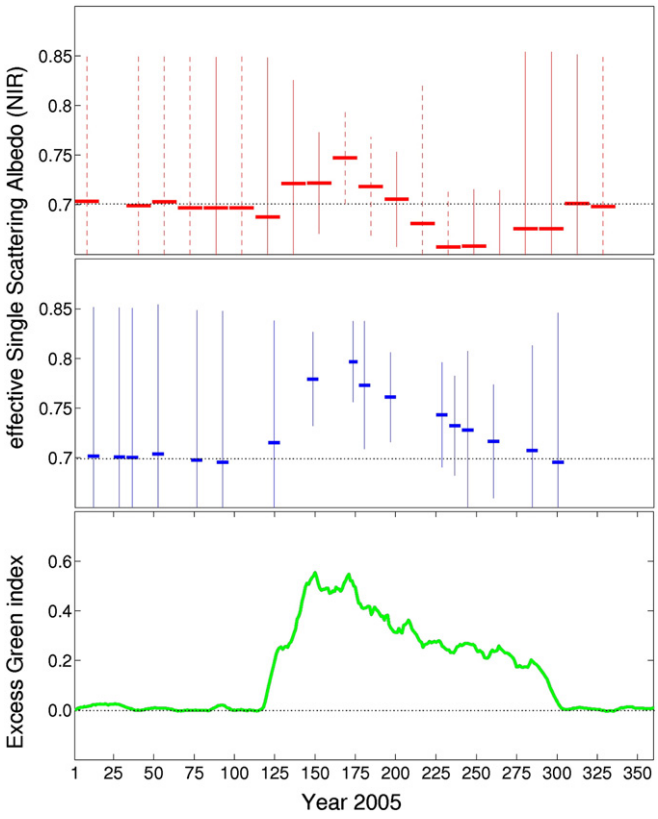

Fig. 6. Time series of the Excess Green index (green) derived from the Hainich tower camera and the effective single scattering albedo retrieved in the near-infrared domain from MODIS (red) and MISR (blue), respectively. The horizontal dotted line identifies the mean value of the prior PDF associated with the effective single scattering albedo. The full (dashed) vertical bars indicate the one-sigma posterior uncertainty associated with the best (good) quality MODIS input albedos. The Excess Green index values have been scaled between 0.0 and 1.0. (For interpretation of the references to color in this figure legend, the reader is referred to the web version of this article.)

400 m transect over the seven year period. The dark and light shaded zones (blue and red) delineate the interquartile range and the 95% confidence level between the statistical distribution of the two flux fractions, respectively, while the thick horizontal bars correspond to the median values. About half of these difference values (considering the median) fall within the ± 0.10 domain (horizontal dashed lines) while 3/4 of the data set is confined in the ± 0.15 domain (horizontal solid lines). Furthermore, all outliers with respect to this envelope are in the positive domain indicating thus a tendency for the JRC-TIP retrievals to exceed those of the in-situ measurements. This overestimate concerns the dormant season and, in particular, two MISR observations analyzed using snowy background prior conditions as well as the end of the green-up phase at the beginning of May and, perhaps more significantly, the senescence phase in October.

We will focus here on the last two situations in view of their importance for downstream applications. Regarding the green-up phase, one can notice on the top panel in Fig. 2 that the MODIS albedo value in the visible domain is much higher (about twice) at the beginning of May (DOY days 129 to 144) than would be logically expected assuming a smooth variation between the previous and subsequent observations. Decreasing this particular surface albedo value by about 0.02 to make it fit the transition between its neighboring points is enough to significantly improve the situation regarding the JRC-TIP and in-situ estimates of the transmitted flux. We thus presume that this observation is an outlier. This is by contrast with the situation occurring during the senescence phase where larger deviations between the JRC-TIP and the in-situ estimates, are consistently observed from MISR and especially MODIS albedos. As noted in Section 3.4, such occurrences are accompanied by a decrease in the effective LAI concurrent with changes in the scattering properties of the canopy. Both features are identified from the JRC-TIP retrievals and lead, together with an underestimate of the effective LAI, to an overestimate of the transmitted fraction of light to the canopy floor.

The middle panel of Fig. 8 displays the time series of the difference between the absorbed (A) and intercepted ($1-T$) fractions of radiation in the visible domain as delivered by the JRC-TIP baseline processing. This panel thus displays this difference under an ideal scenario ensuring that both the intercepted and absorbed fluxes are accurately balanced as is the case when using the JRC-TIP retrievals. This contrasts with the seasonal variation of this difference observed when replacing the transmitted flux fraction retrieved from the JRC-TIP with the actual values estimated from in-situ LAI-2000 measurements along the 400 m transect (Fig. 8, bottom panel). The changes between the middle and bottom panel mirror the lack of consistency or correct balancing between the absorbed fraction derived from JRC-TIP baseline processing and the intercepted fraction estimated from in-situ LAI-2000 measurements. Variations shown in the bottom panel emphasize the consequences of the under-estimation by the JRC-TIP of the actual canopy interception during the senescence phase also characterized by simultaneous changes in the scattering properties of the vegetation layer. Nevertheless, 3/4 of the observed intercepted fraction fall within the ± 0.15 range, a value close to the interquartile range estimated between the two statistical distributions.

3.6. Analysis of the retrieved canopy transmission in the senescence phase

In order to analyze conditions prevailing at the end of the senescence phase in more detail, the JRC-TIP was used to perform a sensitivity experiment for which results are summarized in Table 2. This experiment focuses on the scenario occurring at the beginning of October (DOY 273 to 288) where the fraction of transmitted flux retrieved from the JRC-TIP with MODIS albedos significantly overestimates the one derived from in-situ measurements collected on DOY 283 of year 2005. The first column gives the values corresponding to the JRC-TIP baseline processing that has been used to generate the MODIS derived products at global scale. These are the values discussed so far in the present investigation. Experiment 2 is the same as the baseline but with a drastic increase *i.e.*, a factor of ten, in the precision of the observed albedos. Experiments 3 was performed with an observation data set that includes simultaneously both the MODIS albedos and the in-situ canopy transmission estimated from the LAI-2000 in the visible domain (both data sets are shown on the top panel of Fig. 3) associated with a one-sigma value of 0.1. Experiment 4 is essentially the same as experiment 3 but with a higher uncertainty on the in-situ canopy transmission *i.e.*, the one-sigma value is increased from 0.1 to 0.3. Both experiments were conducted using strong constraints on the precision of the observed albedos *i.e.*, 0.5% as imposed in experiment 2.

A remarkable point from these results concerns the excellent capability of the JRC-TIP to reconstruct the complete observational data set (MODIS surface albedos and in-situ transmission together) that is, generating posterior PDFs almost identical to those observed for all the cases. This good fit is achieved with low values of the cost function. It implies that the in-situ transmission data set is not incompatible with the space-derived albedo values even when increasing the observational constraints through the adoption of very stringent conditions regarding the precision of the observations. One cannot thus identify the quality of the MODIS and MISR surface albedo products as the cause of the departure of the JRC-TIP baseline transmission retrievals from the in-situ estimates.

The posterior information on the retrieved model parameters remain essentially unchanged between experiments 1 and 2 suggesting that there is a limited benefit beyond a very significant improvement in the precision of the albedo observations. By constrast the addition of the transmitted flux in the observational data set, as done in

Please cite this article as: Pinty, B., et al., Evaluation of the JRC-TIP 0.01° products over a mid-latitude deciduous forest site, *Remote Sensing of Environment* (2011), doi:10.1016/j.rse.2011.08.018

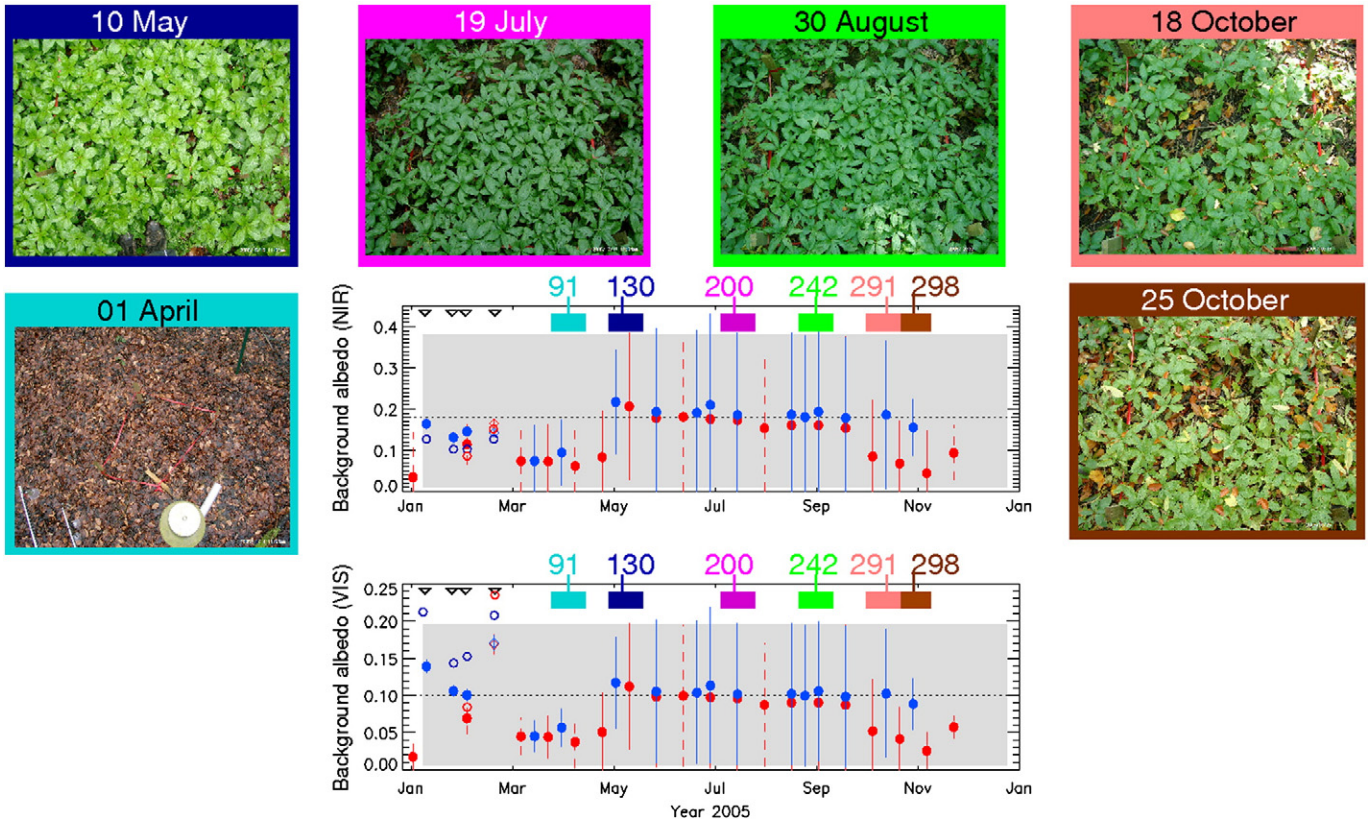

Fig. 7. Time series of the background albedo inferred in the near-infrared (top panel) and visible (bottom panel) estimated by the JRC-TIP. Symbols and color coding are the same as in Fig. 2. The shaded zones delineate the one-sigma prior uncertainty values. The full (dashed) vertical bars indicate the one-sigma posterior uncertainty associated with the best (good) quality MODIS input albedos. Open symbols are for the mean of the PDFs retrieved assuming a snowy background at dates identified by triangles on the top axis. Top view photos of the ground are displayed in the upper part of the figure. The dates of the photos are color coded and identified in the two inside panels.

experiments 3 and 4, translates into much higher effective LAI values as required to account accurately for this extra information. This is also accompanied by an increase (decrease) in the effective scattering albedo of the vegetation layer in the visible (near-infrared) domain in order to fit the surface albedo observations *i.e.*, a decrease in the absorption (scattering) efficiency in the visible (near-infrared) domain. Finally, given the high effective LAI values retrieved with experiments 3 and 4, the background albedo values remain unchanged from their prior values. Reducing the observational precision on the transmitted flux (from experiments 3 to 4) mainly translates into higher uncertainties on the retrieved effective LAI but does not alter significantly the mean value of its wide PDF that tends to get closer to its prior value set at 1.5. It is noteworthy that the observational data set used as input to the JRC-TIP to run experiments 3 and 4 provides an efficient manner to document the pixel-domain averaged radiative characteristics of the Hainich forest site, including those that are difficult to access from in-situ measurements. This generic approach can also be applied to any other site where similar in-situ observations representative of domain-averaged values are available.

In the absence of constraints from the transmitted flux, the JRC-TIP baseline retrievals (first column) are associated with high uncertainties reflecting the large extension of the parameter space that can provide good solutions to Eq. (1). The sensitivity study demonstrates that this is a consequence of insufficient relevant information in the surface albedo observations. There is indeed a large number of solutions to interpret the radiation escaping the canopy in the upward direction. Significant efforts are required to evaluate the overall benefits of using more advanced but also more uncertain products than the spectrally and angularly integrated white sky albedos *e.g.*, bi-directional reflectances or directional albedos, in addressing this particular issue globally at 0.01° resolution. By contrast, adding time constraints in the retrieval procedure may prove to be a relevant approach given that it would limit the strong decrease experienced by the effective LAI with JRC-TIP baseline processing at the start of the senescence phase (Lewis et al., submitted for publication). For global applications it may however raise other issues such as those related to the occurrence of sudden changes in the surface properties due for instance to burning, flooding, clearing or even rapid green-up events. The respective advantages and limitations of such a temporal approach remain, however to be thoroughly evaluated.

4. Discussion of the evaluation procedure

The current evaluation of the JRC-TIP 0.01° spatial resolution products over the Hainich forest site has been conducted using retrievals from one single pixel that is, without performing any spatial averaging. The agricultural fields surrounding the Hainich forest site undergo a growing phase associated with a greening which, on average, follows that of the forest but at a slightly faster rate. They however exhibit a quite different temporal pattern from the forest following the harvesting period (end of June/beginning of July). Fig. 9 displays the time-series of the fractions of transmitted and absorbed visible radiation generated by the JRC-TIP over each of the 8 MODIS pixels (in grey) surrounding the central one associated with the Hainich site (in red). This radiant flux exhibits about the same seasonal pattern at all locations including the partial contamination by snow and clouds. Our estimates at the central pixel tend however to slightly strenghten the deviations from the in-situ measurements (assuming they are representative of the conditions prevailing at all 9 pixels) during both the green-up and the senescence phases. Although it is possible that some observed MODIS and MISR albedos at the target location are affected by the agricultural fields, there is little evidence that this is actually the case from Fig. 9.

Please cite this article as: Pinty, B., et al., Evaluation of the JRC-TIP 0.01° products over a mid-latitude deciduous forest site, *Remote Sensing of Environment* (2011), doi:10.1016/j.rse.2011.08.018

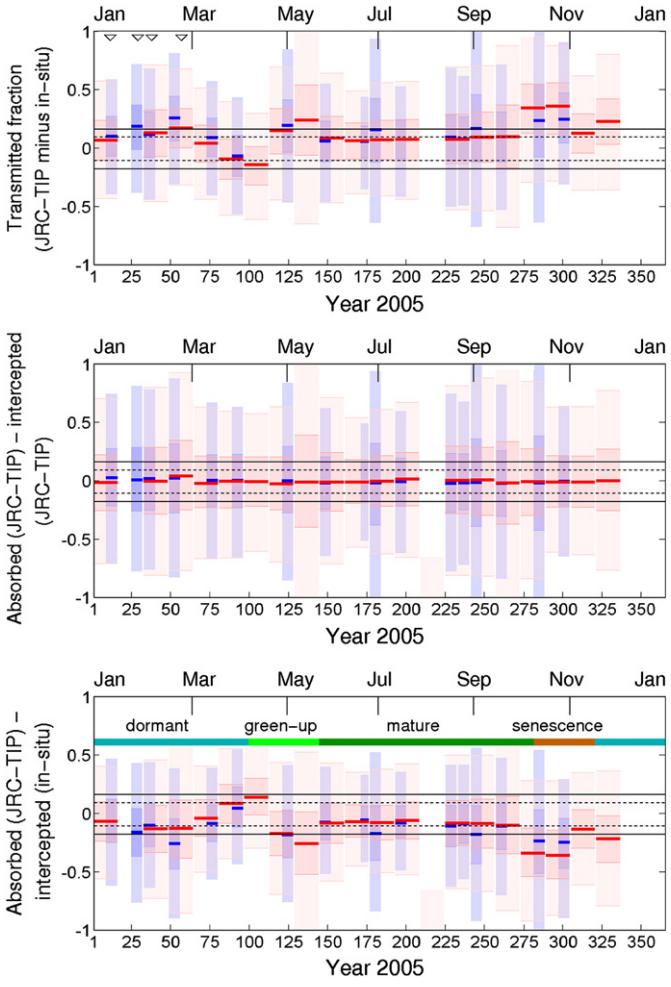

Fig. 8. Time series of the differences between various fractions of radiation in the visible domain. The dark and light shaded zones delineate the interquartile range and the 95% confidence level between the statistical distribution of the two flux fractions. The thick line corresponds to the median value. The red and blue tones identify the retrievals using MODIS (16-day period) and MISR (8-day period) surface albedos as inputs to the JRC-TIP, respectively. Top panel: using the transmitted fractions delivered by the JRC-TIP and the in-situ LAI-2000 measurements along the 400 m transect. Middle panel: based on the JRC-TIP retrievals only. Bottom panel: based on the intercepted fractions estimated from in-situ LAI-2000 measurements along the 400 m transect. (For interpretation of the references to color in this figure legend, the reader is referred to the web version of this article.)

The comparison of the statistical distributions generated from the in-situ measurements and the JRC-TIP is at the core of the evaluation exercise. As discussed in Section 2.5, the range of the in-situ derived estimates is dominated by the sub-pixel/domain spatial variability of the forest. Deriving accurate and precise estimates from the ensemble of local measurements is thus rather challenging. The JRC-TIP delivers PDFs based on pixel/domain-averaged input values, *e.g.*, MODIS and MISR 0.01° resolution surface albedo products. The order of magnitude of the one-sigma values of the retrieved PDFs generated for the fractions of transmitted and absorbed fractions is about the same as that of the range of the ground-based estimates in many instances but much larger than the corresponding interquartile ranges.

These uncertainties estimated by the JRC-TIP rise notably, in relative terms, when estimating the effective LAI both from space and in-situ observations (assuming ± 0.05 uncertainty on the transmitted flux) collected during the growing and maturity seasons *i.e.*, effective LAI values higher than about 1.5. Beyond this value, the JRC-TIP retrievals of the effective LAI from the broadband surface albedos are rather imprecise given that the effective LAI tends to reach its upper limit of useful inference between 3.0 and 4.0. As discussed in (Pinty et al., 2010a, see Fig. 7) this precision can be improved by increasing the constraints on the prior values, in particular, the effective single scattering of vegetation *e.g.*, considering a 'green' leaf scenario (see Table 1). The 'green' leaf scenario constrains the observed albedos to be interpreted by the two-stream model as if all vegetation scattering elements behaved like healthy green leaves that is, exhibiting a high scattering efficiency in the near-infrared domain. This scenario does not yield very different mean values from the 'standard' case when the retrieved vegetation single scattering albedo corresponds to green leaves *e.g.*, during the growing and maturity stages. It however suggests an earlier onset of the senescence than observed in Fig. 5 from the standard scenario. The standard scenario is indeed able to recover part of the deviations from typical green healthy leaves. In the former case that is with imposed 'green' leaves, the decrease in the observed near-infrared albedos has to be balanced by lower effective LAI values in order to reduce the contribution from the vegetation layer and to interpret the signal as observed. The impact of such considerations on downstream applications that ingest fraction of absorbed photosynthetically active radiation products derived from satellite observations has to be evaluated (see for instance, Knorr et al., 2010; Beer et al., 2010).

We have operated a specific version of the JRC-TIP to express the measured transmission at each location along the 400 m transect in terms of effective LAI. The uncertainties associated with the effective LAI values that are retrieved from the observed transmission reflect the propagation of the observational uncertainties *i.e.*, ± 0.05 in the present case, the uncertainty related to the radiation transfer model *i.e.*, a few percent relative, and the uncertainty arising from the radiation transfer regimes *e.g.*, the saturation of the intercepted fraction. Uncertainty values in the 1.5–2.0 range for large, but not extreme, effective LAI may be close to a floor value given that they are associated with 1) rather optimistic uncertainties on the observations and, 2) measurements corresponding to angularly integrated quantities and one may expect the uncertainty to rise when considering solar angle dependency. The additional contribution caused by internal variability makes it thus very challenging to derive precise estimates of pixel/domain-averaged effective LAI values even from in-situ observations of transmitted radiation. Any transformation of the effective LAI into a 'true' and even a 'green' LAI requires additional information in particular about the canopy structure at the pixel/domain resolution (see for instance, Breda, 2003; Chen et al., 1997b, 2005; Jonckheere et al., 2004). It remains however that the uncertainty associated with this additional sub-pixel/domain information (canopy structure and leaf color) must be quantified and propagated adequately to the end product. These issues exemplify the tremendous difficulties related to the validation of such advanced LAI products generated globally from medium resolution spaceborne sensors. One possible avenue to provide a more complete evaluation of the JRC-TIP products would be the use of 3-D radiation transfer models that simulate both the in-situ and the JRC-TIP retrievals for deterministic (as opposed to statistical) representations of 3-D vegetation canopies (http://rami-benchmark.jrc.ec.europa.eu).

The series of photographs taken on site complements the in-situ measurements and is unique in documenting the behavior of the changes in the vegetation if not soil properties. The latter could be evaluated using ground-based devices with the appropriate spatial sampling such that pixel/domain-averaged values could be reliably estimated. This would greatly help as well during winter and spring seasons when partial contamination by snow is a challenging issue but also for an eventual assessement of the quality of the input albedo products *i.e.*, the MODIS and MISR albedo biases were found to propagate to the background albedo under low effective LAI conditions. The quantitative evaluation of the scattering properties of the vegetation is very difficult and would require some dedicated instrumentation on the tower. This evaluation is however quite an important task to accomplish as this model parameter is the main process parameter driving the observed MODIS and MISR albedos when the vegetation is dense enough. In the absence of such quantitative information, the various pictures taken from the top of the tower are

Please cite this article as: Pinty, B., et al., Evaluation of the JRC-TIP 0.01° products over a mid-latitude deciduous forest site, *Remote Sensing of Environment* (2011), doi:10.1016/j.rse.2011.08.018

Table 2
JRC-TIP retrievals from a sensitivity experiment with respect to the observation space. Δ_{λ_1} and Δ_{λ_2} correspond to the broadband visible (0.3–0.7 μm) and near-infrared (0.7–3.0 μm) spectral domains, respectively. $R(\Delta_{\lambda_{1,2}})$ denote the spectral surface albedos while $\omega_l(\Delta_{\lambda_{1,2}})$ and $r_g(\Delta_{\lambda_{1,2}})$ refer to the spectral effective canopy single scattering albedos and background albedos, respectively.

Variable	Exp1[a]	Exp2	Exp3	Exp4
Observational set up[b]				
	No $T(\Delta_{\lambda_1})$	No $T(\Delta_{\lambda_1})$	With $\overline{T(\Delta_{\lambda_1})} = 0.1$[c]	With $\overline{T(\Delta_{\lambda_1})} = 0.1$[c]
$\sigma_{R_{obs}(\Delta\lambda_{1,2})}$[d]	5%[e]	0.5%[e]	0.5%[e]	0.5%[e]
$\sigma_{T_{obs}(\Delta\lambda_1)}$[d]	N/A	N/A	0.1[f]	0.3[f]
Cost function	0.2927	0.2936	0.4161	0.4018
Posterior information in the observation space				
$R(\Delta_{\lambda_1})$	0.0280 ± 0.0014	0.0280 ± 0.0001	0.0280 ± 0.0001	0.0280 ± 0.0001
$R(\Delta_{\lambda_2})$	0.2053 ± 0.0103	0.2050 ± 0.0010	0.2050 ± 0.0010	0.2050 ± 0.0010
$T(\Delta_{\lambda_1})$	0.4083 ± 0.3064	0.4095 ± 0.3007	0.1083 ± 0.0924	0.1413 ± 0.2362
Posterior information in the parameter space				
LAI[g]	1.1721 ± 1.099	1.1679 ± 1.075	3.2358 ± 1.375	2.8092 ± 2.671
$\omega_l(\Delta_{\lambda_1})$[g]	0.1051 ± 0.063	0.1050 ± 0.063	0.1231 ± 0.020	0.1208 ± 0.026
$r_g(\Delta_{\lambda_1})$	0.0521 ± 0.070	0.0518 ± 0.069	0.0934 ± 0.096	0.0893 ± 0.100
$\omega_l(\Delta_{\lambda_2})$[g]	0.6759 ± 0.178	0.6762 ± 0.177	0.5931 ± 0.045	0.5944 ± 0.050
$r_g(\Delta_{\lambda_2})$	0.0849 ± 0.137	0.0844 ± 0.136	0.1652 ± 0.200	0.1563 ± 0.209

[a] Value corresponding to the JRC-TIP baseline processing.
[b] In addition to the observed MODIS albedos: $R(\Delta_{\lambda_1}) = 0.0280$ and $R(\Delta_{\lambda_2}) = 0.2050$.
[c] Mean value of the observed PDF of $T(\Delta_{\lambda_1})$.
[d] Standard deviation values used to set the diagonal of the covariance matrix $\mathbf{C_d}$.
[e] Value relative to the surface albedo observations.
[f] Absolute value.
[g] Effective value.

essential to assess the quality of the retrieved JRC-TIP values. The excellent agreement between temporal variations in the retrieved effective single scattering albedo near-infrared values from MISR and the Excess Green index has to be consolidated with additional investigations at other sites.

The exploitation of the broadband MODIS or MISR surface albedos by the JRC-TIP yields the generation of five model process parameters (the spectrally invariant effective LAI and two parameters related to the spectral scattering properties of the vegetation and the background, respectively) and six radiation fluxes (spectral albedo at the top of the canopy, absorbed fluxes in the vegetation and ground layers, respectively). The current evaluation focuses exclusively on the visible domain due to the lack of appropriate in-situ measurements for instance in the broadband near-infrared domain. Accordingly, only two of these fluxes *i.e.*, the fraction transmitted through and the absorbed by the vegetation layer, can be tentatively assessed in the visible domain where strong absorption in the vegetation layer allows us to approximate, within some limits, the absorbed by the intercepted flux. Such conditions are not satisfied in the near-infrared domain and the evaluation of the corresponding products represents a more challenging task than in the visible domain.

5. Concluding remarks

This paper compares in-situ estimates of the transmitted radiation in the visible domain acquired by LAI-2000 devices to results obtained with the baseline version of the JRC-TIP at 0.01° resolution over the forested site of Hainich. These field measurements were collected systematically and over multiple years through the same 400 m transect. They thus provide quantitative estimates of the subpixel/domain variability and document the temporal changes of the radiant fluxes associated with the various phenological phases of the forest. A series of photographs taken at the top and the bottom of the forest gives additional information complementing those available from the LAI-2000 measurements. Daily time-series of the fractions of transmitted and absorbed fluxes as well as effective LAI were generated with the help of a statistical model increasing thus the coincidence between the in-situ estimates of these products and those delivered by the JRC-TIP baseline processing. The overall agreement between the two sources of data proved to be quite good, both showing the anticipated patterns along a full seasonal cycle including thus the dormant, green-up, maturity and senescence phases. The latter was shown to be rather challenging given the concurrent changes in both the effective LAI and the scattering efficiency of the vegetation *e.g.*, the yellowing of the canopy. Although the JRC-TIP baseline products indicate that both model parameters are covarying as suggested by pictures of the canopy, we also demonstrated that the information contained in the broadband visible and near-infrared domains is too limited to solve this problem precisely. However, the JRC-TIP values associated with this phase are generated with large uncertainty values which allow the onset of the senescence to be identified to some degree.

The case by case analysis of the product values available from the JRC-TIP and the in-situ estimates suggests that two of the MODIS and four of the MISR albedos available during the dormant season were not entirely snow free while two other MODIS albedo observations were probably partially contaminated by clouds: these cases induce sudden but unrealistic variations in the time profiles of the studied variables, variations that are not confirmed by the pictures taken on the Hainich site. As a matter of fact, the use of a snowy background as a prior condition in the former case provided a relevant correction to the JRC-TIP products yielding smoother temporal profiles as expected over this forested site. As a result 3/4 of JRC-TIP retrievals of the transmitted fraction were found to fall within the ± 0.15 uncertainty range when compared with in-situ local measurements. Similar performance is obtained with the absorbed fraction when approximating the latter by the intercepted fraction. The agreement between the two sources of estimates could potentially be improved by considering contributions from pixels surrounding the central location we focused on. This however would not help much exploring limitations intrinsic to the data sets such as those related to the information content of the broadband visible and near-infrared albedos and the use of time and space independent retrievals and priors in the generation of global scale products.

Using contemporaneous MODIS and MISR albedo observations was essential in deriving more complete time-series than is permitted by one sensor only. We could as well assess how the differences in albedo values derived from these two sensors propagate to the JRC-TIP retrievals. For the conditions we studied here, biased low albedo values

Please cite this article as: Pinty, B., et al., Evaluation of the JRC-TIP 0.01° products over a mid-latitude deciduous forest site, *Remote Sensing of Environment* (2011), doi:10.1016/j.rse.2011.08.018

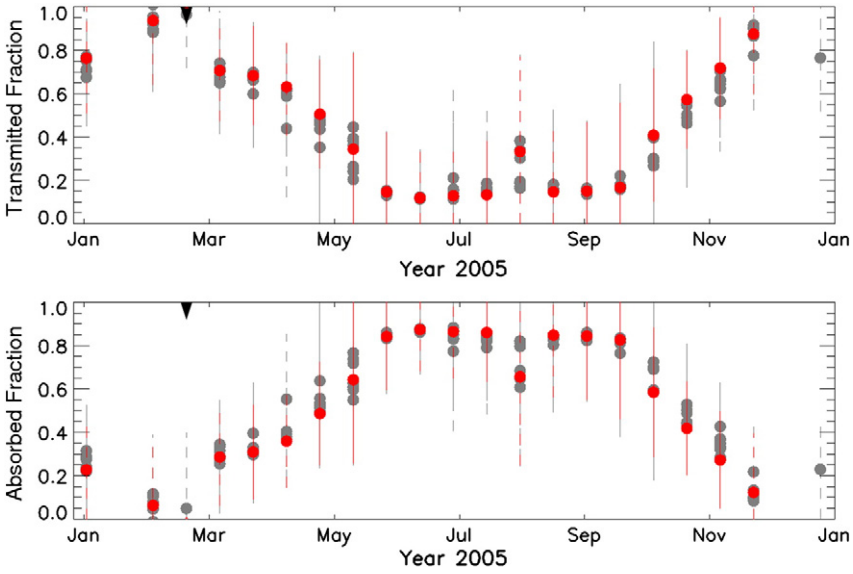

Fig. 9. Time series of the fraction of the transmitted (top panel) and absorbed (bottom panel) radiation in the visible domain over each of the 8 pixels (in grey) surrounding the central one associated with the Hainich site (in red). The full (dashed) vertical bars indicate the one-sigma posterior uncertainty associated with the best (good) quality MODIS input albedos. Triangles on the top axis mark snow events according to the 0.01° resolution MODIS snow flag. (For interpretation of the references to color in this figure legend, the reader is referred to the web version of this article.)

in both spectral bands yield biased high values in the estimate of the transmitted flux. Under dense (sparse) canopy conditions the albedo differences translate into differences in the retrieved effective single scattering albedo of vegetation (albedo of the background). The high sensitivity of the input albedo, and thus the JRC-TIP products, to contaminations by traces of ephemeral snow and local clouds provides a way to evaluate *a posteriori* the performance of the indicators associated with these undesired events.

This contribution highlights the challenging issues and difficulties related to the estimation of in-situ measurements representative of the domain corresponding to the nominal pixel size (and exact location) of the medium spatial resolution sensors. The subpixel variability translates into a range of values that is at least of the same order of magnitude as the uncertainties associated with the JRC-TIP retrievals. Nevertheless the series of LAI-2000 measurements collected over the same 400 m transect over multiple years greatly helped to derive time-series of the fraction of transmitted radiation in the visible domain. The pictures taken on site also proved very relevant to assess the quality of the derived information in particular those related to the changes in canopy and background optical properties. Such an approach is rather simple but efficient to provide a first evaluation of the JRC-TIP baseline products at 0.01° spatial resolution and will be extended to other Fluxnet sites offering similar facilities. The availability of in-situ domain-averaged measurements of the background albedo in both the visible and near-infrared spectral domains would also be valuable. A critical and challenging aspect still concerns the in-situ estimates of the effective vegetation scattering properties that are parameters controlling the observed albedos as well as the retrieved radiant fluxes in the near-infrared domain. A first step has been taken in that direction in estimating a greenness index from the series of photos available from a digital camera monitoring the top of the canopy. The excellent agreement between such an index and the effective single scattering albedo in the near-infrared domain retrieved from MISR indicates that the JRC-TIP retrievals behave according to expectations.

Acknowledgments

This research was performed jointly in the Global Environment Monitoring unit of the Institute for Environment and Sustainability at the Joint Research Centre, an institution of the European Commission and at the Earth Observation Directorate of the European Space Agency. Bernard Pinty acknowledges the support of the Science, Applications and Future Technologies Department of the European Space Agency. The authors are thankful to Ulrich Pruschitzki and Waldemar Ziegler for gathering the LAI-2000 measurements. Galina Churkina kindly provided access to the Ikonos image. Special thanks to Monica Robustelli and Hugo Simoes for their technical and graphical support.

References

Baldocchi, D. D., & Collineau, D. (1994). The physical nature of solar radiation in heterogeneous canopies: Spatial and temporal attributes. In M. Caldwell, & R. Pearcy (Eds.), *Exploitation of environmental heterogeneity by plants* (pp. 21–71). San Diego CA: Academic Press.

Beer, C., Reichstein, M., Tomelleri, E., Ciais, P., Jung, M., Carvalhais, N., et al. (2010). Terrestrial gross carbon dioxide uptake: Global distribution and covariation with climate. *Science*, *329*, 834–838.

Breda, N. J. J. (2003). Ground-based measurements of Leaf Area Index: A review of methods, instruments and current controversies. *Journal of Experimental Botany*, *54*, 2403–2417.

Breiman, L. (1996). Bagging predictors. *Machine Learning*, *24*, 123–140.

Breiman, L. (2001). Random forests. *Machine Learning*, *45*, 5–32.

Chen, J. M., Blanken, P. D., Black, T. A., Guilbeault, M., & Chen, S. (1997). Radiation regime and canopy architecture in a boreal Aspen forest. *Agricultural and Forest Meteorology*, *86*, 107–125.

Chen, J. M., Govind, A., Sonnentag, O., Zhang, Y., Barr, A., & Amiro, B. (2006). Leaf Area Index measurements at Fluxnet-Canada forest sites. *Agricultural and Forest Meteorology*, *140*, 257–268.

Chen, J. M., Menges, C. H., & Leblanc, S. G. (2005). Global mapping of foliage clumping index using multi-angular satellite data. *Remote Sensing of Environment*, *97*, 447–457.

Chen, J. M., Rich, P. M., Gower, S. T., Norman, J. M., & Plummer, S. (1997). Leaf area index of boreal forests: Theory, techniques, and measurements. *Journal of Geophysical Research*, *102*, 29429–29443.

Clerici, M., Voßbeck, M., Pinty, B., Kaminski, T., Taberner, M., Lavergne, T., et al. (2010). Consolidating the Two-stream Inversion Package (JRC-TIP) to retrieve land surface parameters from albedo products. *IEEE Journal of Selected Topics in Earth Observations and Remote Sensing*, *2*.

De Kauwe, M. G., Disney, M. I., Quaife, T., Lewis, P., & Williams, M. (2011). An assessment of the MODIS collection 5 leaf area index product for a region of mixed coniferous forest. *Remote Sensing of Environment*, *115*, 767–780.

Gamon, J. A., Cheng, Y., Claudio, H., MacKinney, L., & Sims, D. A. (2006). A mobile tram system for systematic sampling of ecosystem optical properties. *Remote Sensing of Environment*, *103*, 246–254.

Gausman, H. W., & Allen, W. A. (1973). Optical parameters of leaves of 30 plant species. *Plant Physiology*, *52*, 57–62.

Gobron, N., Pinty, B., Aussedat, O., Chen, J. M., Cohen, W. B., Fensholt, R., et al. (2006). Evaluation of FAPAR products for different canopy radiation transfer regimes: Methodology and results using Joint Research Centre products derived from SeaWiFS against

ground-based estimations. *Journal of Geophysical Research*, *111*, D13110, doi: 10.1029/2005JD006511.

Hufkens, K., Richardson, A. D., & Friedl, M. (2011). Monitoring species specific phenology with conventional RGB cameras. *Proceedings of the European Geophysical Union, Vienna, Austria, 04–08 April 2011*. : European Geophysical Union.

Jonckheere, I., Fleck, S., Nackaerts, K., Muys, B., Coppin, P., Weiss, M., et al. (2004). Review of methods for in situ leaf area index determination. Part I. theories, sensors and hemispherical photography. *Agricultural and Forest Meteorology*, *121*, 19–35.

Knapp, A. K., & Carter, G. A. (1998). Variability in leaf optical properties among 26 species from a broad range of habitats. *American Journal of Botany*, *85*, 940–946.

Knorr, W., Kaminski, T., Scholze, M., Gobron, N., Pinty, B., Giering, R., et al. (2010). Carbon cycle data assimilation with a generic phenology model. *Journal of Geophysical Research*, *115*, G04017, doi:10.1029/2009JG001119.

Kutsch, W. L., Kolle, O., Rebmann, C., Knohl, A., Ziegler, W., & Schulze, E. -D. (2008). Advection and resulting CO_2 exchange uncertainty in a tall forest in central Germany. *Ecological Applications*, *18*, 1391–1405.

Law, B. E., Cescatti, A., & Baldocchi, D. D. (2001). Leaf area distribution and radiative transfer in open-canopy forests: Implications for mass and energy exchange. *Tree Physiology*, *21*, 777–787.

Lewis, P., Gomez-Dans, J., Kaminski, T., Settles, J., Quaife, T., Gobron, N., Styles, J., & Berger, M. (submitted for publication). An Earth Observation Land Data Assimilation System (EO-LDAS). *Remote Sensing of Environment*.

Martonchik, J. V., Diner, D. J., Pinty, B., Verstraete, M. M., Myneni, R. B., Knyazikhin, Y., et al. (1998). Determination of land and ocean reflective, radiative, and biophysical properties using multiangle imaging. *IEEE Transactions on Geoscience and Remote Sensing*, *36*, 1266–1281.

McNeil, B. E., Denny, E., & Richardson, A. D. (2008). Coordinating a northeast regional phenology network. *Bulletin of the Ecological Society of America*, *89*, 188–190.

Morisette, J. T., Baret, F., Privette, J. L., Myneni, R. B., Nickeson, J. E., Garrigues, S., et al. (2006). Validation of global moderate resolution LAI products: a framework proposed within the CEOS Land Product Validation subgroup. *IEEE Transactions on Geosciences and Remote Sensing*, *44*, 1804–1817.

Morisette, J. T., Nightingale, J., & Nickeson, J. (2010). An international workshop on the validation of satellite-based phenology products. *EOS Transactions of the American Geophysical Union*, *91*, 407–408.

Morisette, J. T., Richardson, A. D., Knapp, A. K., Fisher, J. I., Graham, E. A., Abatzoglou, J., et al. (2009). Tracking the rhythm of the seasons in the face of global change: Phenological research in the 21st century. *Frontiers in Ecology and the Environment*, *7*, 253–260.

Mund, M., Kutsch, W. L., Wirth, C., Kahl, T., Knohl, A., Skomarkova, M. V., et al. (2010). The influence of climate and fructification on the interannual variability of stem growth and net primary productivity in an old-growth, mixed beech forest. *Tree Physiology*, *30*, 689–704.

Nolan, V. P., & Weltzin, J. F. (2011). Phenology for science, resource management, decision making, and education. *EOS Transactions of the American Geophsyical Union*, *92*, 15.

Ollinger, S. V., Richardson, A. D., Martin, M. E., Hollinger, D. Y., Frolking, S. E., Reich, P. B., et al. (2008). Canopy nitrogen, carbon assimilation, and albedo in temperate and boreal forests: Functional relations and potential climate feedbacks. *Proceedings of the National Academy of Sciences of the United States of America*, *105*, 19335–19340.

Pinty, B., Andredakis, I., Clerici, M., Kaminski, T., Taberner, M., Verstraete, M. M., et al. (2010). Exploiting the MODIS albedos with the Two-stream Inversion Package (JRC-TIP) Part I: effective Leaf Area Index, Vegetation and Soil properties. *Journal of Geophysical Research*, *116*.

Pinty, B., Clerici, M., Andredakis, I., Kaminski, T., Taberner, M., Verstraete, M. M., et al. (2010). Exploiting the MODIS albedos with the Two-stream Inversion Package (JRC-TIP) Part II: Fractions of transmitted and absorbed fluxes in the vegetation and soil layers. *Journal of Geophysical Research*, *116*.

Pinty, B., Gobron, N., Widlowski, J. -L., Lavergne, T., & Verstraete, M. M. (2004). Synergy between 1-D and 3-D radiation transfer models to retrieve vegetation canopy properties from remote sensing data. *Journal of Geophysical Research*, *109*.

Pinty, B., Lavergne, T., Dickinson, R. E., Widlowski, J. -L., Gobron, N., & Verstraete, M. M. (2006). Simplifying the interaction of land surfaces with radiation for relating remote sensing products to climate models. *Journal of Geophysical Research*, *111*.

Pinty, B., Lavergne, T., Kaminski, T., Aussedat, O., Giering, R., Gobron, N., et al. (2008). Partitioning the solar radiant fluxes in forest canopies in the presence of snow. *Journal of Geophysical Research*, *113*.

Pinty, B., Lavergne, T., Voßbeck, M., Kaminski, T., Aussedat, O., Giering, R., et al. (2007). Retrieving surface parameters for climate models from MODIS and MISR albedo products. *Journal of Geophysical Research*, *112*.

Pinty, B., Lavergne, T., Widlowski, J. -L., Gobron, N., & Verstraete, M. M. (2009). On the need to observe vegetation canopies in the near-infrared to estimate visible light absorption. *Remote Sensing of Environment*, *113*.

Pinty, B., Widlowski, J. -L., Verstraete, M. M., Andredakis, I., Arino, O., Clerici, M., et al. (2010). Snowy backgrounds enhance the absorption of solar radiation in forest canopies. *Geophysical Research Letters*, *38*.

Reifsnyder, W. E., Furnival, G. M., & Horowitz, J. L. (1971). Spatial and temporal distribution of solar radiation beneath forest canopies. *Agricultural Meteorology*, *9*, 21–37.

Reithmaier, L. M., Gockede, M., Markkanen, T., Knohl, A., Churkina, G., Rebmann, C., et al. (2006). Use of remotely sensed land use classification for a better evaluation of micrometeorological flux measurement sites. *Theoretical and Applied Climatology*, *84*, 219–233.

Richardson, A., Braswell, B. H., Hollinger, D. Y., Jenkins, J. P., & Ollinger, S. (2009). Near-surface remote sensing of spatial and temporal variation in canopy phenology. *Ecological Applications*, *19*, 1417–1428.

Richardson, A., Jenkins, J. P., Braswell, B. H., Hollinger, D. Y., Ollinger, S., & Smith, M. -L. (2007). Use of digital webcam images to track spring green-up in a deciduous broadleaf forest. *Oecologia*, *152*, 323–334.

Roberts, D. A., Nelson, B. W., Adams, J. B., & Palmer, F. (1998). Spectral changes with leaf aging in Amazon caatinga. *Trees-Structure and Function*, *12*, 315–325.

Schaaf, C. B., Gao, F., Strahler, A. H., Lucht, W., Li, X., Tsang, T., et al. (2002). First operational BRDF, albedo and nadir reflectance products from MODIS. *Remote Sensing of Environment*, *83*, 135–148.

Taberner, M., Pinty, B., Govaerts, Y., Liang, S., Verstraete, M. M., Gobron, N., et al. (2010). Comparison of MISR and MODIS land surface albedos: Methodology. *Journal of Geophysical Research*, *115*.

Voßbeck, M., Clerici, M., Kaminski, T., Pinty, B., Lavergne, T., & Giering, R. (2009). An inverse radiative transfer model of the canopy based on automatic differentiation. *Inverse Problems*, *26*.

Voßbeck, M., Giering, R., & Kaminski, T. (2008). Development and first applications of TAC++. In C. Bischof, H. M. Bücker, P. D. Hovland, U. Naumann, & J. Utke (Eds.), *Advances in Automatic Differentiation* (pp. 189–197). Springer.

Widlowski, J. -L. (2010). On the bias of instantaneous FAPAR estimates in open-canopy forests. *Agricultural and Forest Meteorology*, *150*, 1501–1522.

Woebbecke, D., Meyer, G. E., Von Bargen, K., & Mortensen, D. A. (1995). Color indices for weed identification under various soil residue and lighting conditions. *Transactions of ASAE*, *38*(1), 259–269.

Please cite this article as: Pinty, B., et al., Evaluation of the JRC-TIP 0.01° products over a mid-latitude deciduous forest site, *Remote Sensing of Environment* (2011), doi:10.1016/j.rse.2011.08.018